Journal of Human Evolution 114 (2018) 85–101

Contents lists available at ScienceDirect

Journal of Human Evolution

journal homepage: www.elsevier.com/locate/jhevol

Scaling of bony canals for encephalic vessels in euarchontans: Implications for the role of the vertebral artery and brain metabolism

Doug M. Boyer*, Arianna R. Harrington

Department of Evolutionary Anthropology, Duke University, Durham, NC, 27708, USA

ARTICLE INFO

Article history:
Received 20 December 2016
Accepted 2 September 2017
Available online 31 October 2017

Keywords:
Cognition
Metabolic scaling
Internal carotid artery
Vertebral artery
Encephalization quotient
Allometry

ABSTRACT

Supplying the central nervous system with oxygen and glucose for metabolic activities is a critical function for all animals at physiologic, anatomical, and behavioral levels. A relatively proximate challenge to nourishing the brain is maintaining adequate blood flow. Euarchontans (primates, dermopterans and treeshrews) display a diversity of solutions to this challenge. Although the vertebral artery is a major encephalic vessel, previous research has questioned its importance for irrigating the cerebrum. This presents a puzzling scenario for certain strepsirrhine primates (non-cheirogaleid lemuriforms) that have reduced promontorial branches of the internal carotid artery and no apparent alternative encephalic vascular route except for the vertebral artery. Here, we present results of phylogenetic comparative analyses of data on the cross-sectional area of bony canals that transmit the vertebral artery (transverse foramina). These results show that, across primates (and within major primate subgroups), variation in the transverse foramina helps significantly to explain variation in forebrain mass even when variation in promontorial canal cross-sectional areas are also considered. Furthermore, non-cheirogaleid lemuriforms have larger transverse foramina for their endocranial volume than other euarchontans, suggesting that the vertebral arteries compensate for reduced promontorial artery size. We also find that, among internal carotid-reliant euarchontans, species that are more encephalized tend to have a promontorial canal that is larger relative to the transverse foramina. Tentatively, we consider the correlation between arterial canal diameters (as a proxy for blood flow) and brain metabolic demands. The results of this analysis imply that human investment in brain metabolism (~27% of basal metabolic rate) may not be exceptional among euarchontans.

1. Introduction

Some of the most intriguing and debated questions in evolutionary biology are those surrounding the evolution and scaling of brain size (Jerison, 1955, 1973; Martin, 1981; Armstrong, 1983, 1985; Dunbar, 1998; Pagel, 2002; Finarelli and Flynn, 2007; Isler et al., 2008; Grabowski, 2016; Grabowski et al., 2016). Relatedly, researchers have long sought to understand the cognitive benefits (Van Valen, 1974; Willerman et al., 1991; Dunbar, 1998; Deaner et al., 2007; Shettleworth, 2009; Hofman, 2014; Krupenye et al., 2016; MacLean, 2016) and energetic costs of a large brain (Pagel and Harvey, 1988; Aiello and Wheeler, 1995; Dunbar, 1998; Isler and Van Schaik, 2006; Weisbecker and Goswami, 2010; Karbowski, 2011; Navarrete et al., 2011; Isler, 2013; Seymour et al., 2015, 2016; Pontzer et al., 2016). In this study, we address the question of how, anatomically, brains maintain adequate blood perfusion. We do so using comparative data on cross sectional areas of bony canals for arteries capable of irrigating the brain, hereafter referred to as encephalic arteries.[1]

Among primates and their close euarchontan relatives, the encephalic arteries primarily include (1) the vertebral arteries, which originate from the subclavian arteries and ascend through the transverse foramina of the sixth through first cervical vertebrae, and (2) branches of the carotid arteries. In many taxa, encephalic branches of the carotid arteries anastomose with the basilar artery (formed by fusion of the vertebral arteries) in the circle of Willis (Fig. 1).

[1] Note that encephalic arteries are a type of cranial artery. Non-encephalic, cranial arteries include those associated with the cranium that do not necessarily supply brain tissue. The stapedial artery, which branches from the internal carotid artery in some taxa, and meningeal arteries can be considered non-encephalic, cranial arteries.

* Corresponding author.
E-mail address: doug.boyer@duke.edu (D.M. Boyer).

http://dx.doi.org/10.1016/j.jhevol.2017.09.003
0047-2484/

Unlike the vertebral arteries, which ubiquitously contribute to encephalic circulation, euarchontans show several different configurations in their carotids. Scandentians (non-primate euarchontans, a.k.a. treeshrews), anthropoids, and tarsiers rely on an internal carotid vessel that travels to the brain via the promontorial canal (Bugge, 1974; Cartmill and MacPhee, 1980; MacPhee, 1981; MacPhee and Cartmill, 1986; Boyer et al., 2016). Certain other euarchontans involute (i.e., lose ontogenetically)

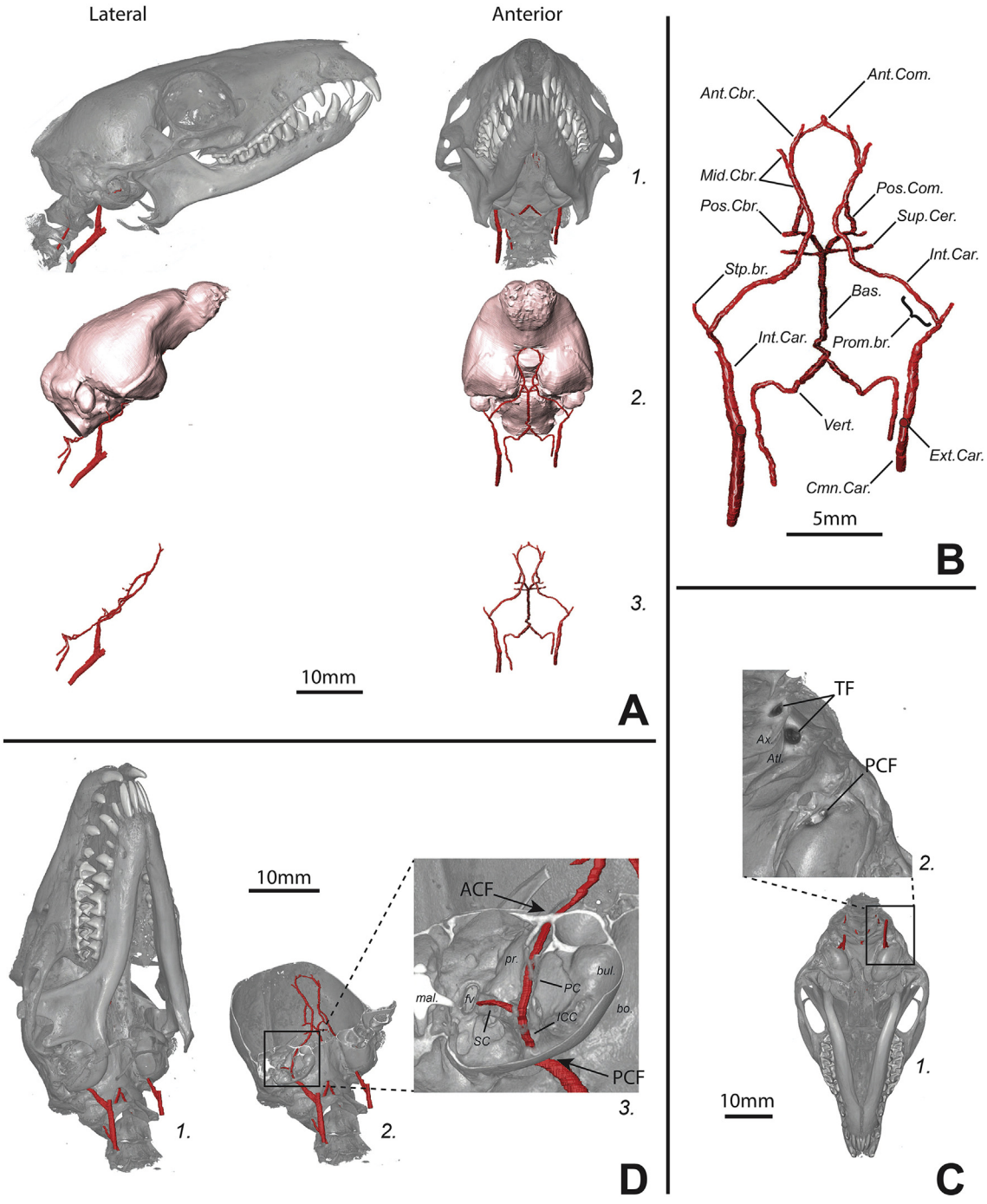

Figure 1. Diagram of encephalic blood supply. This study focuses on understanding the role of the vertebral artery in cerebral and encephalic blood supply and on predicting the metabolic energy consumption of the brain using estimates of the brain size and encephalic arterial canal diameter. **A***(1)*, microCT rendering of a *Tupaia* skull in lateral and anterior view. **A**(*2*), bone removed to show segmentation of the endocranial cast (which approximates brain volume, mass and morphology) and encephalic vasculature. **A**(*3*), endocranial cast removed to show arterial segmentation. This specimen retained alcohol-preserved soft tissue. The vascular system was perfused with latex and the dilated arterial lumen were traced using ImageJ and Avizo 8.1. **B**, detail of encephalic vasculature lumen casts showing the major components of the arterial circle of Willis. The pattern in haplorhine primates and humans is almost identical. Abbreviations: Ant, Anterior; Bas, Basilar; br, branch; Car, Carotid; Cbr, Cerebral; Cer, Cerebellar; Cmn, Common; Com, Communicating; Ext, External; Int, Internal; Mid, Middle; Pos, Posterior; Prom, Promontorial; Stp, Stapedial; Sup, Superior; Vert, Vertebral. **C***(1)*, microCT rendering of skull in ventral view**. C***(2)*, inset of microCT rendering of skull showing transverse foramen (TF) in atlas (Atl) and axis (Ax), as well as posterior carotid foramen (PCF) between petrosal and entotympanic. **D***(1)*, microCT rendering of skull in ventrolateral view. **D***(2)*, cut away to show tympanic cavity and endocranium. **D***(3)*, inset showing details of tympanic cavity. Abbreviations: ACF, anterior carotid foramen; bo, basioccipital; bul, bulla (entotympanic); fv, fenestra vestibule; ICC, internal carotid canal; mal, malleus; PC, promontorial canal (measured to represent promontorial artery); PCF, posterior carotid foramen; pr, promontorium of petrosal; SC, stapedial canal.

the internal carotid artery and rely on external carotid branches as adults. Specifically, cheirogaleid lemuriforms have an enlarged ascending pharyngeal artery that enters the cranium through the foramen lacerum (Cartmill, 1975). Lorisids have a similar pattern except that the ascending pharyngeal sometimes forms an extracranial rete mirable (a diffuse arterial network) before entering (Cartmill, 1975). Dermopterans (non-primate euarchontans a.k.a. 'flying lemurs') also have an external carotid-derived rete mirable, but it enters the endocranium through the superior orbital fissure (Wible, 1993). Finally, non-cheirogaleid lemuriforms involute the promontorial branch of the internal carotid artery without developing a compensating external carotid branch. However, the involution process is incomplete in some adult individuals, in which a small amount of blood flow is still possible through the promontorial route (Bugge, 1974; Conroy and Wible, 1978). Thus, it is thought that the vertebral arteries are the sole irrigators of the brain in non-cheirogaleid lemuriforms (Conroy, 1982).

In this study, we wish to better understand brain irrigation among taxa with differently configured encephalic vascular anatomy. Specifically, we use measurements of the transverse foramina and the promontorial canals to evaluate whether the vertebral arteries contribute significantly to cerebral (forebrain) blood requirements, whether there are clade level differences in the encephalic blood requirements between haplorhine and strepsirrhine primates, and whether the configuration of the brain's irrigation system affects brain size and/or structure. We then explore the potential for using data on encephalic arterial canals and brain size to predict the metabolic energy consumption of the brain.

Operationally, we organize our study around three hypotheses:

1) Interspecific variation in forebrain blood requirements is primarily managed and reflected by the carotid arteries, except in certain strepsirrhine primates that have evolutionarily lost all carotid contributions to the encephalic system. An important corollary to this hypothesis is that the vertebral arteries are primarily adapted to meet vascular demands of the hindbrain.
2) Cognitive differences among different groups of euarchontans are associated with different mass-specific blood flow requirements of their neural tissue.
3) Total encephalic arterial flow rate reflects brain metabolic energy demands.

The first hypothesis is based upon previous studies that experimentally measure volumetric rate of blood flow in the internal carotid and vertebral arteries. These studies tend to find that flow volumes in the vertebral artery are low compared to the carotids (Baldwin and Bell, 1963; Schöning et al., 1994; van Bel et al., 1994; Scheel et al., 2000; Turnquist and Minugh-Purvis, 2012). Despite being composed of a far greater number of neurons, the cerebellum is argued to require less blood than the cerebrum due to the much lower energetic cost of a cerebellar neuron compared to a cerebral neuron (Karbowski, 2007; Herculano-Houzel, 2011; Strominger et al., 2012; Seymour et al., 2015). Therefore, the finding that flow volumes are low in the vertebral arteries has been interpreted (Seymour et al., 2015) to indicate that the vertebral arteries primarily supply the 'low cost' hindbrain structures (cerebellum, medulla, and pons), despite their anastomoses with the internal carotid arteries in the circle of Willis. Relatedly, the higher flow volumes measured for internal carotid arteries are thought to reflect involvement in forebrain irrigation (Coceani and Gloor, 1966; Reneman et al., 1974; Wellens et al., 1975; Tatu et al., 1996, 1998; Scremin, 2011). Two recent studies (Seymour et al., 2015, 2016) have operationalized these results and equated total cerebral blood flow to volume rate of flow in the internal carotid artery. However, the accuracy of this proposed equivalence is questioned by the fact that non-cheirogaleid strepsirrhines must utilize the vertebral artery for forebrain blood supply. Might the vertebral artery also provide significant amounts of blood to the forebrain, albeit to a lesser extent, in other primates?

To test the hypothesis that blood supply to the forebrain can be modeled without considering the vertebral artery in some primates, we evaluate the prediction that only the cross sectional area of the promontorial canal for the internal carotid artery significantly correlates with forebrain size (Boyer et al., 2016). The cross-sectional area of the bony canal for the vertebral artery (transverse foramen) should remain uncorrelated with forebrain size if it is unimportant for estimating forebrain blood requirements.

The next hypothesis, that cognitive differences among groups of primates are reflected by differences in forebrain blood requirements, is based on the findings of Seymour et al. (2015, 2016) that internal carotid flow rates increase with brain size at the fastest rate (i.e., with the steepest slope) in extant and fossil hominins, at an intermediate rate in anthropoids, and at a much lower rate in marsupials. Seymour et al. (2015) interpret their findings according to the argument that blood volume rate of flow can be taken as equivalent to metabolic energy consumption (Hawkins et al., 1983; Schmidt-Nielsen, 1984; Lou et al., 1987; Changizi, 2001; Karbowski, 2011) and that the metabolic cost of neural tissue is affected by the neuronal density of that tissue (Karbowski, 2007; Herculano-Houzel, 2011; Fonseca-Azevedo and Herculano-Houzel, 2012) as well as the size, interconnectivity, and firing rate of its neurons (Karbowski, 2007; Strominger et al., 2012; Magistretti and Allaman, 2015). In other words, Seymour et al. (2015, 2016) interpret metabolic demands as a function of neural tissue architecture and cellular processes.

Therefore, Seymour et al. (2015, 2016) suggest that their blood flow scaling results reflect the observation that anthropoids (and other primates) maintain a higher neuronal density with increasing brain size compared to other mammals (Herculano-Houzel et al., 2015). They also use their results to propose the hypothesis that tissue-specific costs of the brain were driven up during hominin evolution by increasing neuron interconnectivity and synaptic activity as required to support greater cognitive ability/complexity. While blood flow rates may well reflect metabolic energy consumption and neuronal properties, Seymour et al.'s (2015, 2016) estimates of cerebral flow scaling are questionable for several reasons. These include the difficulty in modeling flow rates from canal diameters (see our sensitivity analysis: Supplementary Online Material [SOM] S1), Seymour et al.'s (2015, 2016) use of internal carotid foramen size alone to model the rate of blood flow to the forebrain, and their use of variance in endocranial volume as a proxy for variance in forebrain volume.

Given these methodological limitations, we note at least two alternative possible explanations (other than differences in cerebral metabolic activity) for observed exponent differences among marsupials, anthropoids and hominins. First, if the forebrain actually receives blood from both the internal carotid and vertebral arteries in certain taxa, then exponents measured by Seymour et al. (2015, 2016) using the carotid alone could bias the results in specific ways. In particular, there may well be an allometrically shifting reliance by the forebrain from more vertebral blood in smaller brains to more internal carotid blood in larger ones. Saban (1963) hinted at this possibility when noting that humans exhibit a larger carotid canal relative to the vertebral canal than taxa with smaller brains. Under this scenario, the forebrain flow to some of

Table 1
Taxon list and species mean values.

Species	nTFA	nPA	DTFA	DPA	ACA	ECV	BM	BMR	Source
Hominoidea									
Gorilla gorilla[a]	8	3	65.85	26.77	92.61	455.89	71,500	–	1
Homo sapiens[a]	10	3	68.69	91.12	159.81	1422.33	65,000	1557	1,3
Hylobates lar[a]	5	3	11	13.71	24.71	100.49	5381	–	1
Pan troglodytes[a]	6	3	41.61	28.13	69.74	343.49	37,133	1307	2,3
Pongo pygmaeus	9	3	57.62	24.03	81.65	368	36,948	1037	1,3
Cercopithecoidea									
Macaca fascicularis	5	2	9.8	8.81	18.61	63.06	3884	251.9	1,2
Mandrillus leucophaeus	2	2	22.63	12.64	35.27	160	17,500	–	1
Miopithecus talapoin[a]	7	3	7.09	3.62	10.71	39.08	1877	–	1
Papio anubis[a]	10	2	23.46	14.81	38.27	152.45	13,300	435.4	1,2
Lophocebus albigena[a]	7	2	13.54	8.87	22.41	97.99	7890	–	1
Nasalis larvatus[a]	6	1	15.56	8.8	24.36	83.84	9730	–	1
Piliocolobus badius[a]	5	2	10.32	13.57	23.88	64.49	7850	–	1
Platyrrhini									
Alouatta sp.[a]	21	3	16.3	7.04	23.34	52.75	5753	231.9	1,4
Aotus trivirgatus[a]	10	1	6.07	2.49	8.56	16.85	989	52.86	1,2
Ateles geoffroyi[a]	4	3	17.13	13.68	30.81	106.59	7453	–	1
Cacajao calvus	3	1	12.2	6.8	19	76	2935	–	1
Callicebus moloch[a]	7	2	5.15	2.75	7.9	17.78	1070	–	1
Callithrix jacchus	7	3	3.2	1.14	4.34	7.43	318	22.8	1,4
Callithrix pygmaea[a]	6	1	2.02	0.72	2.74	4.02	110	10.1	1,4
Cebus capucinus[a]	7	2	8.94	6.03	14.98	67.02	2436	–	1
Chiropotes satanas	3	3	8.2	7.76	15.96	48.33	2132	–	2
Pithecia pithecia	3	1	5.69	3.15	8.85	32.26	1760	–	1
Saimiri sciureus[a]	9	2	6.08	2.86	8.94	24.6	799	68.51	1,2
Tarsiidae									
Tarsius sp.[a]	5	4	1.47	0.54	2.01	3.27	109	8.89	1,2
Lemuriformes (Cheirogaleidae)									
Cheirogaleus major[a]	2	2	2.93	0.21	3.14	5.81	140	–	1
Cheirogaleus medius[a]	2	1	1.61	0.09	1.7	2.6	400	22.47	1,2
Microcebus murinus[a]	5	2	0.73	0.04	0.78	1.63	65	–	1
Mirza sp.	1	2	1.8	0.08	1.88	5.75	312	–	1
Lemuriformes (non-Cheirogaleidae)									
D. madagascariensis[a]	3	3	11.17	0.77	11.94	45.31	2555	–	1
Archaeolemur majori	5	3	38.97	0.8	39.76	93	18,200	–	1
Avahi laniger[a]	5	2	5.81	0.17	5.99	9.86	1206	–	1
Babakotia radofilai	2	2	25.54	0.71	26.26	48	16,000	–	1
Hapalemur griseus	6	2	7.06	0.15	7.20	14.04	689.50		1
Indri indri[a]	2	2	16.5	0.48	16.98	35.9	6335	–	1
Propithecus verreauxi[a]	4	2	11.88	0.26	12.14	30.06	2955	86.8	1,4
Eulemur fulvus ssp.[a]	7	3	9.36	0.22	9.58	23.06	2210	42	1,4
Lemur catta	8	3	10.68	0.27	10.94	22.9	2210	45.1	1,4
Prolemur simus	3	1	10.65	0.24	10.89	27.14	2150	–	1
Varecia sp.[a]	3	3	11.53	0.34	11.87	32.15	3497	69.9	1,4
Lepilemur sp.[a]	4	3	4.52	0.11	4.63	8.21	691	27.6	1,4
Lorisiformes									
Galago senegalensis[a]	9	3	1.76	0.05	1.82	3.97	196	–	1
Otolemur crassicaudatus[a]	8	2	3.58	0.25	3.82	12.25	1170	47.3	1,2
Loris tardigradus[a]	3	2	1.88	0.11	2	5.87	193	13.65	1,2
Nycticebus coucang[a]	8	2	5.39	0.19	5.58	11.01	679	35.95	1,2
Perodicticus potto[a]	8	2	5.78	0.15	5.93	12.81	802	59.05	1,2
Non-primates (Dermoptera)									
Cynocephalus volans	1	3	4.02	0.24	4.27	5.78	810	–	1
Galeopterus variegatus	4	2	2.88	0.20	3.07	6.78	1330	–	1
Non-primates (Scandentia)									
Ptilocercus lowii	1	3	1.08	0.21	1.3	1.67	43	4.99	1,2
Tupaia glis	9	3	1.15	0.38	1.54	3	142	10.78	1,2

Abbreviations: nTFA & nPA = number of individuals for which transverse foramina diameters and promontorial canal diameters were measured; DTFA = doubled transverse foramen cross sectional area (CSA, in mm^2), to represent the sum of the CSA of the vertebral arteries on the right and left sides; DPA = doubled promontorial canal CSA (in mm^2), to represent the sum of the CSA of the internal carotid arteries on the right and left sides; ACA = the sum of DTFA and DPA; ECV = endocranial volume (in mL); BM = body mass (in g); BMR = basal metabolic rate (in Kcal/day); *D.* = *Daubentonia*. All DTFA values were calculated from data measured in this study. DPA, ECV, BM, and BMR were derived from sources 1 = Boyer et al. (2016); 2 = McNab (2008), and 3 = Pontzer et al. (2016); 4 = Leonard et al. (2003).

[a] Denotes taxa with brain component values available from Stephan et al. (1981; see SOM Table S6). See Table S3 of specimen-level data of measurements of TFA.

the smaller primate brains may have been under-predicted by Seymour et al. (2015), which could explain some unexpected overlap with marsupials. Even if all forebrain flow is captured by the internal carotid artery, there is a second factor that could lead to over-estimating exponents of forebrain flow, which stems from treating endocranial volume as a proxy for forebrain size: allometry of forebrain-hindbrain ratios. Forebrain-hindbrain ratios are correlated with brain size among euarchontans, with larger brains having a larger forebrain relative to the hindbrain.[2] Therefore, if

[2] Analyzing correlation between endocranial volume and forebrain–hindbrain ratios with data from Stephan et al. (1981) returns a significant positive correlation (df = 32, Pagel's lambda = 0.963, F = 4.7, $p = 0.03641$).

Table 2
Taxa with total arterial canal area (ACA), endocranial volume (ECV), and whole Brain Glucose Utilization rates (Glucose Util.). Data used for predicting glucose utilization from ECV and/or ACA.

Species	Glucose util. (μmol/min)	Source (Karbowski, 2007)	ACA (mm^2)[a]	ECV (cc)	ECV source	Neuron count
Homo sapiens	428.55	Clarke and Sokoloff, 1994	159.81	1422.33	Boyer et al., 2016	8.606E+10
Macaca	35.98	Kennedy et al., 1978	18.61	87.3	H-H et al., 2007	6.376E+09
Mus	0.32	Bouilleret et al., 2000	0.32	0.402	H-H et al., 2011	6.787E+07
Oryctolagus	7.93	Passero et al., 1981	9.66	9.132	H-H et al., 2011	4.942E+08
Rattus	1.52	Nehlig et al., 1988	1.82	1.724	H-H et al., 2011	1.889E+08
Sciurus	3.88	Frerichs et al., 1995	3.46	5.548	H-H et al., 2011	4.537E+08
Papio	60.4	Meguro et al., 1999	38.27	152.5	Boyer et al., 2016	1.095E+10

[a] Arterial canal area (ACA) values are newly available as part of the current study. Karbowski (2007) provides brain metabolism data in SOM Table S1, S2. Endocranial volume (ECV) from Boyer et al. (2016), and Herculano-Houzel et al. (2007, 2011). All neuron count values from Herculano-Houzel et al. (2015).

larger brains typically also have a larger forebrain–hindbrain ratio, they should also have a larger estimated forebrain flow relative to the whole, even if nothing has changed regarding the tissue specific costs of the forebrain.

These problems stemming from vertebral artery contributions to the forebrain and forebrain–hindbrain allometry can be avoided by examining the scaling of total encephalic flow to total brain size. Ideally, to test Seymour et al.'s (2015) hypothesis, we would estimate total encephalic blood flow for the same sample of marsupial and anthropoid species. Unfortunately, such data are currently unavailable. However, a similar goal can be accomplished by comparing certain strepsirrhine primates and anthropoids. Since Seymour et al. (2015) relate the higher slope in anthropoids to cognitively demanding behaviors such as complex sociality, it stands to reason that strepsirrhines, with more rudimentary cognitive abilities (e.g., Sandel et al., 2011; Maille and Roeder, 2012) and a tendency towards less complex sociality (e.g., Dunbar, 1998), should exhibit a more 'normal' mammalian pattern (i.e., a smaller exponent and/or reduced blood demands for a given brain mass). Furthermore, if a trend towards more carotid reliance in bigger brains is at play, we should find consistently larger exponents relating the internal carotid arterial canal to brain size than relating the vertebral arterial canal to brain size. Finally, if increasing encephalization during hominin evolution resulted in increasing carotid dominance over the vertebral artery, we might expect a broader correlation between carotid dominance and encephalization (or relative brain size) among Euarchonta. Alternatively, carotid dominance may actually reflect higher forebrain–hindbrain ratios (Conroy, 1982).

The third hypothesis we aim to test here is that blood volume rate of flow meaningfully reflects energetic costs. While we agree with the literature (cited above) establishing that blood flow rate should be (on balance) linearly correlated with metabolic energy consumption, arterial flow scaling rates are extremely sensitive to several parameters that must be estimated, including arterial wall thickness and vessel wall shear stress (SOM S1). Furthermore, it is also possible that high interspecific variance in recruitment of anaerobic metabolism by the brain (Bauernfeind et al., 2014) or in blood oxygen and glucose content (Vaishnavi et al., 2010) could obscure the relationship between blood flow and brain metabolism.

To test this hypothesis, while avoiding issues associated with predicting flow rates from canal diameters, our approach is to compare total encephalic arterial canal area, brain size, and neuron counts to see which of these variables expresses a significant relationship with whole brain metabolic energy consumption. If arterial canal cross-sectional areas meaningfully reflect brain metabolic demands, then they should be significantly correlated with measured brain metabolic energy consumption after controlling for brain size and neuron count. We think this is a potentially useful endeavor even though cellular processes of neural tissue form the most direct cause of brain metabolism. There are at least two reasons why this endeavor is useful. First, cellular level processes are not necessarily straightforward to model despite some claims that brain metabolism is a simple linear product of neuron count (Herculano-Houzel, 2011). Second, even if cell-level measurements are ultimately more informative indicators of brain metabolism than are dimensions of encephalic arterial canals and/or brain size, there are many extant and fossil taxa for which soft tissue will never be available.

2. Materials and methods

2.1. Sample and measurements

The primary novel data for this study are measurements reflecting the major and minor cross-sectional axes of the transverse foramina of the first and second cervical vertebrae, which transmit the vertebral arteries (Fig. 1D). While measuring artery cross sections directly would have been preferable, this is infeasible due to lack of adequate samples of fresh or perfused cadavers. For some analyses, these data were combined with data reflecting cross-sectional dimensions of the internal carotid canal or – in taxa that have a stapedial artery branching from the internal carotid after it enters the skull – its promontorial segment from Boyer et al. (2016).[3] We evaluated these canal data in the context of published data on mass of specific brain parts (Stephan et al., 1981), brain/endocranial volume (Herculano-Houzel et al., 2007, 2011; Isler et al., 2008; Herculano-Houzel and Kaas, 2011; Boyer et al., 2016), brain metabolic energy consumption (Karbowski, 2007, 2011), whole body basal metabolic rate (Kleiber, 1947; Leonard et al., 2003; McNab, 2008; Tacutu et al., 2013; Pontzer et al., 2016), body mass (Smith and Jungers, 1997; Herculano-Houzel et al., 2007, 2011; Herculano-Houzel and Kaas, 2011; Boyer et al., 2016), and whole brain neuron counts (Herculano-Houzel et al., 2007, 2011; Herculano-Houzel and Kaas, 2011).

The sample includes 53 species (Table 1, Table 2), including fossil and extant primates, dermopterans, scandentians, and gliroids (n = 287 individuals; SOM Table S3). Species were chosen to comprehensively reflect the superorder Euarchonta. As much as possible, we used the same species as in Boyer et al. (2016) for the promontorial canal. In some cases, we needed to add species not included in Boyer et al.'s study, in which case we followed their methods when collecting new data. Specifically, *Pan troglodytes* and

[3] The internal carotid canal of species that retain a stapedial artery and/or stapedial canal into adulthood is not equivalent to the internal carotid canal of those lacking the stapedial artery: in the former group, the internal carotid artery carries both encephalic and non-encephalic blood, while in the latter it carries only encephalic blood. Therefore, we use the term promontorial canal/artery to refer to a segment of the carotid canal/artery that is always equivalent regardless of the retention of the stapedial canal/artery in carrying only encephalic blood (Fig. 1).

Chiropotes satanas were not included in Boyer et al. (2016) and new data on the diameter of the promontorial canal were collected for these taxa. Data for promontorial-equivalent, internal carotid canals were also newly collected for gliroids noted by Bugge (1974) to rely on both the vertebral and internal carotid arteries for blood supply to the brain: *Mus musculus, Rattus norvegicus*, and *Oryctolagus cuniculus* (Table 2).

Most measurements of the transverse foramina were taken on physical specimens using digital calipers under a dissecting microscope. Some specimens were only available digitally as three-dimensional surface files reconstructed from x-ray CT scans obtained from Morphosource.org and the Kyoto University Primate Research Institute's Digital Morphology Museum website. One digital specimen of *Ptilocercus lowii* was kindly provided by S.G. Chester. The digital specimens were measured using the "2D measurement" tool in Avizo 8.1 (Visualization Sciences Group). The two transverse foramen measurements taken were the maximum foramen diameters along a dorsal–ventral axis and a medial–-lateral axis. Both the right and left transverse foramina of the atlas and axis were measured, when available. Measurements were taken by both authors. From these data, cross-sectional areas were calculated as the product of the two transverse foramen diameters. Each cross-sectional area was averaged for the individual before being included into a species average.

For certain analyses (see below), the average transverse foramen cross-sectional area (TFA) for each species was added to the average promontorial canal cross-sectional area (PA) for a "total" cross-sectional area. This "total" cross-sectional area was doubled (as these vessels are bilateral), as were TFA and PA when analyzed on their own. We refer to the "doubled total" cross-sectional as "total arterial canal area" (ACA) in the text below and figures. Endocranial volume (ECV), body mass (BM), doubled TFA (DTFA), doubled PA (DPA), and ACA were natural logarithm transformed prior to analysis.

Species were assigned to one of three brain blood supply route categories based on Bugge (1974) and Cartmill (1975), as reviewed by Boyer et al. (2016). These groups were defined as including taxa that receive blood to the brain either 1) exclusively by the vertebral arteries (non-cheirogaleid lemuriforms), 2) by a combination of the vertebral arteries and the internal carotid arteries (haplorhines and scandentians), or 3) by a combination of the vertebral arteries and the external carotid arteries (cheirogaleid lemuriforms, lorisiforms, and dermopterans). Of the gliroids, *Sciurus carolinensis* was characterized as receiving encephalic irrigation from the vertebral artery only.

An encephalization quotient (EQ) was calculated for each taxon as the difference between the actual ECV and predicted ECV value from a phylogenetic generalized least squares (pGLS) regression [$\ln(ECV) = 0.757^{*}\ln(BM) - 2.565$; $p < 0.0001$, $r^2 = 0.87$] for all extant euarchontan taxa in the sample.

2.2. Analyses

All analyses in this study were done with species mean values. This allowed us to combine datasets from different studies, to avoid pseudo-replication and artificial inflation of sample power, and to utilize phylogenetic comparative methods. Wherever possible, pGLS approaches were utilized. All pGLS analyses used the tree topology and branch lengths of Boyer et al. (2016). Most were executed in the statistical program R with the package Caper (Orme et al., 2011). Phylogenetic ANCOVA was executed in BayestraitsV2 (Pagel and Meade, 2013).

Accuracy of maximum likelihood estimates of phylogenetic signal is intractable for samples less than $n = 20$ taxa (Münkemüller et al., 2012). Therefore, when samples are smaller than 20 degrees of freedom, we present results with lambda set to 1.0. In order to generate a predictive equation with <20 taxa we modify a Bayesian approach developed for 'phylogenetically informed' prediction of trait values (Nunn and Zhu, 2014). This approach allows us to factor in both prediction error and uncertainty in phylogenetic signal. Specifically, we generate a posterior distribution of 1000 regressions relating whole Brain Glucose Utilization (BGU) and two predictor variables (ACA and ECV). This posterior distribution is sampled at rate 0.10, resulting in generation of 99 predictive equations that can be used to generate a posterior distribution of 99 BGU predictions for each taxon. We use these distributions to determine a mean predicted value as well as 95% credibility intervals using the R package BEST.

Correcting alpha levels to avoid type I error is an important concern for this study as we run a number of iterations of each analysis (Sokal and Rohlf, 1995; Abdi, 2007). There is often debate about when and whether a Bonferroni correction is appropriate or overly conservative. In this study, we consider tests of effects on the whole sample (Euarchonta) as sequentially related to tests on phylogenetic and functional subgroups. That is, given a significant result at the level of Euarchonta, the subgroup comparisons are tests of the applicability of these findings to specific clades or functional groups. Furthermore, to avoid overly conservative Bonferroni correction, we use a step-wise alpha correction protocol often called the Dunn-Šidák method (Šidák, 1967).

While applying these correction rates technically changes the pattern of significance in Table 5, rendering one of the correlations non-significant, we note that the hypotheses for these tables are structured such that a non-significant result rejects the null hypothesis. Therefore, it seems to us that the critical value for these tests should actually be increased in order to formally reduce the chance of inflated type I error rate.

2.3. Experimental design and hypothesis testing

The first set of analyses in this study focused on testing the hypothesis that the variation in forebrain demands for blood are reflected in the carotids alone. In other words, that variation in the vertebral arteries is unrelated to functional demands of supplying the forebrain. The primary prediction we address is that the cross sectional areas of the cervical transverse foramina (DTFA) do not explain variance in forebrain size after accounting for variation in promontorial canal cross sectional area (DPA). We evaluated this prediction by running a pGLS multiple regression of DTFA and DPA on ECV. We also check this prediction for subgroups of primates.

We also reverse the dependency of our variables, and evaluate the prediction that forebrain size does not explain variance in DTFA when controlling for BM. We do this by running pGLS multiple regressions of forebrain volume and BM on DTFA. While it would be interesting to run a multiple regression of forebrain volume and hindbrain volume on DTFA, forebrain volume and hindbrain volume are correlated with $r^2 = 0.99$ which is a level of collinearity that is too high for meaningful results (O'brien, 2007).

For this study, the forebrain volume was defined as the combined volumes of the diencephalon and telencephalon, whereas hindbrain volume was defined as the combined volumes of the medulla oblongata and cerebellum. Volume of the mesencephalon was not included in either category due to the likelihood that it would be irrigated more equally by vessels branching from both the internal carotid and vertebral-basilar arteries. Brain part volumes were compiled from Stephan et al. (1981) and reported in SOM Table S6.

Table 3
PGLS Multiple regression of promontorial canal area (DPA) and transverse foramen area (DTFA) on forebrain masses (dependent; first three columns) and hindbrain masses (dependent; last three columns). Each column is the output of one analysis. Only taxa and groups for which the ICA and VA represent all potential encephalic blood routes are included.

	Forebrain			Hindbrain		
	Euarchonta	ICA + VA	VA only	Euarchonta	ICA + VA	VA only
	$n = 26$, df = 23	$n = 19$, df = 16	$n = 7$, df = 4	$n = 26$, df = 23	$n = 19$, df = 16	$n = 7$, df = 4
Intercept						
Mean (±SE)	0.95 (±0.19)	1.19 (±0.28)	1.12 (±0.73)	−0.36 (±0.25)	−0.41 (±0.27)	−0.29 (±0.72)
DPA coeff.						
Mean (±SE)	0.39 (±0.06)	0.69 (±0.10)	0.38 (±0.20)	0.40 (±0.08)	0.54 (±0.10)	0.28 (±0.20)
t Ratio	6.04	7.16	1.91	5.29	5.62	1.40
p (mean = 0)	<0.0001	<0.0001	0.13	<0.0001	<0.0001	0.23
DTFA coeff.						
Mean (±SE)	0.98 (±0.09)	0.60 (±0.12)	0.99 (±0.23)	0.89 (±0.10)	0.73 (±0.12)	0.95 (±0.23)
t Ratio	11.27	5.04	4.22	9.28	6.12	4.14
p (mean = 0)	<0.0001	0.0001	0.01	<0.0001	<0.0001	0.01
Overall stats						
λ	0.54 (ML)	1.0	1.0	0.97 (ML)	1.0	1.0
Adjusted r^2	0.96	0.97	0.96	0.96	0.96	0.95
F ratio	329.55	253.09	77.30	261.21	233.50	63.78

Abbreviations: **Sample:** Euarchonta (all taxa except those with a non-ossifying rete mirable), VA-only (taxa for which the internal carotid supply to the brain is variable or absent and the vertebral artery supplies the bulk of the blood to the brain – non-cheirogaleid lemuriforms), ICA + VA (taxa for which both the internal carotid and vertebral artery supply significant blood – haplorhines and scandentians). See SOM Table S5 for which species were included in each subset. **Variables:** Forebrain (telencephalon + diencephalon of Stephan et al. (1981), see SOM Table S6); DPA (doubled promontorial canal area); DTFA (doubled transverse foramen area); λ, Pagel's lambda – value representing phylogenetic signal of data; df, degrees of freedom; SE, standard error of estimate; p, probability of **zero** value of parameter; adjusted r^2, adjusted coefficient of determination for correlation; ML, maximum likelihood value of Pagel's lambda.

The second hypothesis we address is that cognitive differences in strepsirrhines and haplorhines are reflected in the mass-specific cost of their brain tissue (with lemurs having less expensive brain tissue). Again, this hypothesis stems from the work of Seymour et al. (2015). We take a few approaches here.

Primarily, we evaluate the prediction that the slope and intercept of the line relating ACA to ECV in non-cheirogaleid lemuriforms is different from that of haplorhines. We do this using phylogenetic ANCOVA in which we estimate and test for differences between slopes and intercepts of both groups.

We also assess the ability of ACA to explain variation in ECV, and compare it with that of DPA and DTFA alone. We do this by running three separate bivariate regressions: ACA vs. ECV, DPA vs. ECV, and DTFA vs. ECV. We then compare measures of phylogenetic signal (Pagel's lambda), the residual squared error and coefficient of determination. If there are differences in per unit encephalic blood requirements of strepsirrhines and non-strepsirrhines, there should be no discernible differences among these regressions in the metrics above. However, if different primate groups actually have similar encephalic blood requirements, then Pagel's lambda and residual squared error should be lowest, and coefficient of determination (r^2) and F statistics should be highest, for ACA vs. ECV. We also use phylogenetic ANOVA to make post hoc comparisons of residuals of each functional blood supply group.

Even if the foregoing analyses suggest there is no discernible difference in implied blood requirements of strepsirrhine and haplorhine brains, we are still left with the perplexing pattern of different exponents relating the internal carotid flow to brain size in different groups of primates (Seymour et al., 2015, 2016). One possible explanation is that the vertebral artery contributes more to small brains and less to larger brains. This idea predicts that slope of DPA vs. ECV is higher than that of DTFA vs. ECV. We assess this prediction by comparing mean slopes of canal specific regressions for Euarchonta and subgroups within it.

Another prediction we evaluate is that taxa with relatively bigger brains have greater dominance of the carotid artery relative to the vertebral artery. We do this by multiple regression of EQ, ECV/BM and forebrain volume/hindbrain volume on the ratio of the promontorial canal cross section to the transverse foramen cross section, DPA/DTFA. Like measurement variables, ratios were also natural log transformed prior to analysis.

Finally, we address the hypothesis that encephalic arterial flow reflects total average metabolic energy consumption of the brain. For testing this hypothesis, we represent brain metabolism with Brain Glucose Utilization (BGU) rates (see Table 2). BGU data in Table 2 are transcribed from Karbowski (2007) who compiled the data from a number of earlier sources (Kennedy et al., 1978; Passero et al., 1981; Waschke et al., 1993; Clarke and Sokoloff, 1994; Meguro et al., 1999; Bouilleret et al., 2000; Nehlig and Boyet, 2000; Levant and Pazdernik, 2004).

Instead of trying to calculate flow rates, we test the prediction that ACA explains a significant amount of variation in BGU when accounting for variation in brain size and total number of neurons. We do this by using multiple regression of BGU on ACA, ECV and neuron count. Since only seven species are available for all three measurements, we opted not to use pGLS for these analyses.

3. Results

Hypothesis 1. *Variation in the carotid arteries alone reflects blood demands of the cerebrum*

PGLS multiple regression of DTFA and DPA on forebrain volume shows that DTFA and DPA both explain highly significant amounts of variance in forebrain volume. This is true for analyses of all subgroups except non-cheirogaleid lemuriforms for which DPA is not significant (Table 3).

Likewise, both canals also explain significant variance in hindbrain volume (Table 3). Again, non-cheirogaleid lemuriforms are an exception with no significant relationship of DPA to hindbrain volume. These results hold whether the maximum-likelihood value of Pagel's lambda is used (which is zero for most subgroups) or lambda of 1.0 is used.

Results of multiple regression of forebrain volume and BM on DTFA indicate that both variables contribute to variance in DTFA (Table 4). For non-cheirogaleid lemuriforms, the contribution by forebrain volume has a p-value of 0.1. However, this group has a small sample size.

Table 4
PGLS Multiple regression of body mass and brain-part mass on transverse foramen area (dependent). Each column is the output of one analysis.

	Forebrain				Hindbrain			
	Euarchonta	ICA + VA	VA only	ECA + VA	Euarchonta	ICA + VA	VA only	ECA + VA
	$n = 34$, df = 31	$n = 19$, df = 16	$n = 7$, df = 4	$n = 8$, df = 5	$n = 34$, df = 31	$n = 19$, df = 16	$n = 7$, df = 4	$n = 8$, df = 5
Intercept								
Mean (±SE)	−1.43 (±0.34)	−1.80 (±0.45)	−1.58 (±0.54)	−1.04 (±0.37)	−0.59 (±0.49)	−1.20 (±0.68)	−1.18 (±0.53)	0.36 (±0.36)
Brain mass coeff.								
Mean (±SE)	0.37 (±0.10)	0.25 (±0.10)	0.27 (±0.13)	0.90 (±0.10)	0.46 (±0.11)	0.30 (±0.14)	0.32 (±0.11)	0.96 (±0.10)
t Ratio	3.83	2.34	2.13	9.40	4.13	2.22	2.87	9.92
p (mean = 0)	0.0005	0.03	0.10	0.0002	0.0002	0.04	0.05	0.0001
Body mass coeff.								
Mean (±SE)	0.31 (±0.08)	0.39 (±0.09)	0.39 (±0.11)	0.10 (±0.06)	0.25 (±0.09)	0.35 (±0.11)	0.38 (±0.09)	0.08 (±0.06)
t Ratio	3.94	4.24	3.46	1.72	2.91	3.06	4.19	1.37
p (mean = 0)	0.0004	0.0006	0.03	0.15	0.01	0.01	0.01	0.23
Overall stats								
λ	0.54 (ML)	1.0	1.0	1.0	0.56 (ML)	1.0	1.0	1.0
Adjusted r^2	0.94	0.93	0.98	0.94	0.94	0.93	0.99	0.94
F ratio	243.95	123.88	163.87	53.05	251.90	120.66	236.07	59.04

Abbreviations: **Sample:** Rete (taxa with a non-ossifying rete assisting the vertebral artery with encephalic blood supply – cheirogaleids, lorisiforms, and dermopterans). See Table 3 legend for explanation of other samples. **Variables:** see Table 3 legend for explanation of variables.

Similar results are recovered when analyzing hindbrain volume and BM on DTFA (Table 4). These results hold whether the maximum-likelihood value of Pagel's lambda is used (which is zero for most subgroups) or lambda of 1.0 is used, except in the case of the subgroup representing haplorhines and treeshrews (the 'ICA + VA' group), in which case the p-value rises to ~0.10 when the maximum likelihood value of lambda is used.

Hypothesis 2. *Strepsirrhines and haplorhines have different cerebral blood requirements*

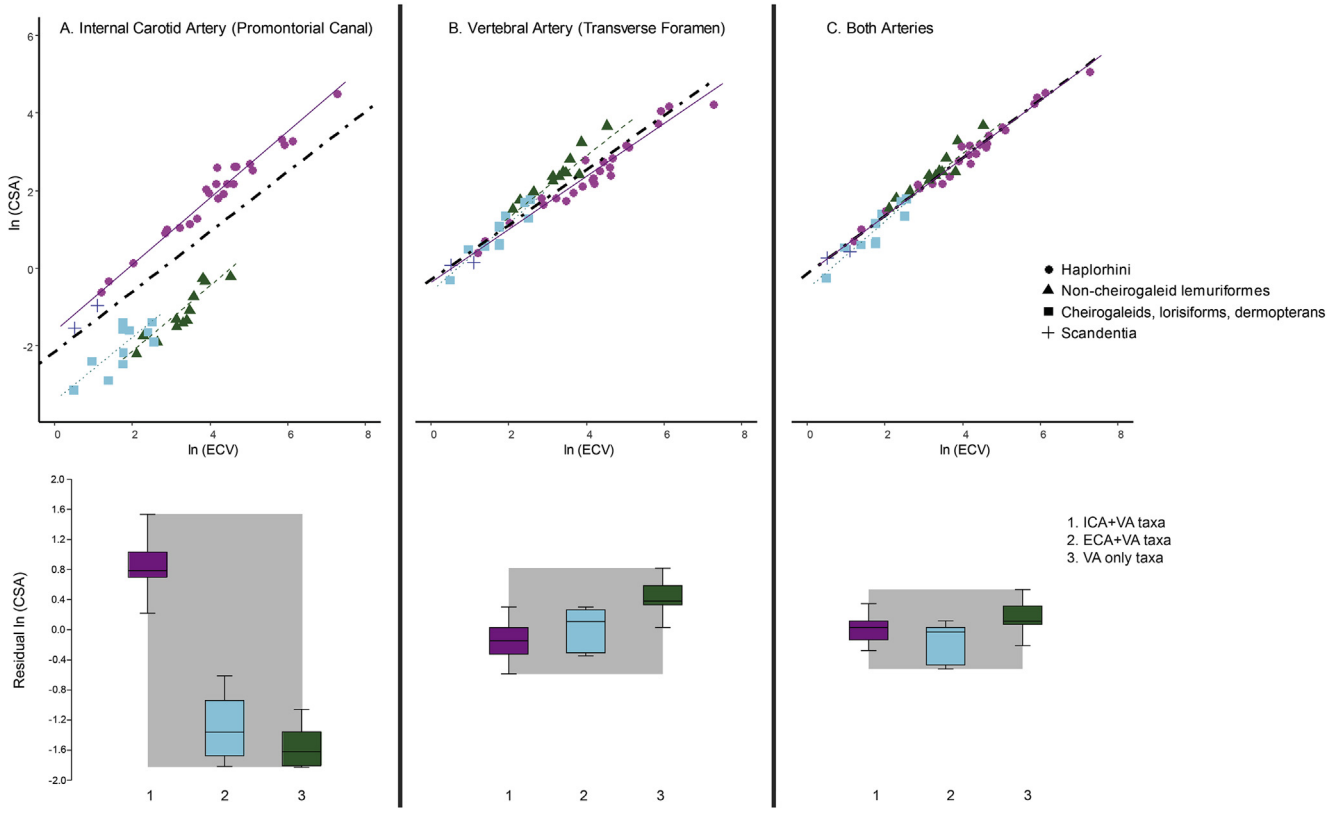

Figure 2. Assessing arterial contribution to encephalic blood supply. All data are natural log transformed and each point represents a species mean value. Statistical analyses were run using phylogenetic generalized least squares. Note that Y-axes are equivalent within a row of images. Therefore, only the left–most axis is labeled. Note that in upper plots the x-axis range is the same for A, B, and C. **A**, Promontorial arterial canal cross sectional area (CSA) v. endocranial volume (ECV) above, residuals by blood supply group below. **B**, Vertebral transverse foramen canal cross sectional area v. ECV above, residuals by blood supply group below. **C**, Total arterial cross sectional area v. ECV above, residuals by blood supply group below. Different lines represent different groups: thick black dashed line = Euarchonta, not including "ECA + VA" taxa defined below; purple solid line = "ICA + VA" taxa relying on the internal carotid and vertebral arteries contribution for brain circulation (haplorhines, scandentians); light blue small dotted line = "ECA + VA" taxa relying on external carotid and vertebral artery contribution for brain circulation (cheirogaleids, lorisiforms, dermopterans); dark green medium dotted line = "VA only" taxa relying only on the vertebral arteries for brain circulation (non-cheirogaleid lemuriforms). All residuals in lower plots were calculated from the thick black dashed line. Gray box represents total residual variation among all subgroups. See Table 5 for equations of the lines and SOM Table S5 for taxa included in each sample. (For interpretation of the references to color in this figure legend, the reader is referred to the web version of this article.)

Results of phylogenetic ANCOVA of ACA vs. ECV in BayestraitsV2 reveals that there are no differences in slope (df = 33, t = 1.05, $p = 0.30$) or intercept (df = 33, t = 0.32, $p = 0.75$) when comparing non-cheirogaleid lemuriforms to haplorhines. This is in contrast to the relationship between DPA vs. ECV, which has strong offsets in intercept, reflecting the reduced internal carotid promontorial canal of strepsirrhines (Boyer et al., 2016).

Bivariate pGLS analyses of ACA vs. ECV, DPA vs. ECV, and DTFA vs. ECV all yield highly significant results (Fig. 2; Table 5). In the regression of ACA vs. ECV, the values of phylogenetic signal (Pagel's lambda) and residual squared error are smaller, while the coefficient of determination (r^2) and F ratio are higher than in the other two analyses. This pattern holds when examining subgroups.

The exponent relating DPA to ECV tends to be higher than that of DTFA to ECV for most groups. This pattern is strongest in carotid reliant taxa (treeshrews and haplorhines), while there are only minimal differences between slopes in the two strepsirrhine functional groups. Strepsirrhines as a whole exhibit a reversed pattern (SOM Table S9), where DTFA has a greater exponent with ECV than does DPA. The 95% confidence intervals on the two sets of relationships overlap except for the comparison of carotid reliant taxa where the 95% minimum exponent for DPA is 0.80, while the 95% maximum for DTFA is 0.74 (Table 5).

When looking at residuals from each of the canal vs. ECV regressions, strepsirrhines deviate significantly from non-strepsirrhines with much more negative DPA residuals, as also shown by Boyer et al. (2016). In reverse, non-cheirogaleid lemuriforms have the most positive residuals of DTFA: they are higher than cheirogaleids, lorisiforms, and anthropoids, which are all groups with alternative routes besides the vertebral artery for supplying the brain (Table 6).

Results of pGLS multiple regression of carotid dominance (DPA/DTFA) on EQ, ECV/BM, and forebrain/hindbrain volume reveals that none of these variables explains a significant amount of variance in carotid dominance at the level of Euarchonta (Table 7). However, the EQ and brain part ratios have much lower p-values than ECV/BM ratios.

Checking the correlation between carotid dominance and each of these variables in a bivariate context actually indicates significant relationships in every case for the sample including all euarchontans (Table 8). When looking at bivariate correlations for subgroups, the ratio of brain size to body size is never significant. The ratio of forebrain to hindbrain volume as well as EQ are both significant for internal carotid reliant taxa (haplorhines and treeshrews). Non-cheirogaleid lemuriforms never express a significant relationship with any variable. However, *Daubentonia* has the largest brain, the largest brain/body ratio, the greatest encephalization, largest promontorial canal, and the greatest carotid canal dominance of any strepsirrhine (Fig. 3).

Hypothesis 3. *Total encephalic arterial canal size reflects brain metabolic demands*

Using data from Table 2, multiple regression of ACA, ECV and neuron count on BGU shows that ACA and ECV explain highly significant amounts of variation in BGU, while neuron count does not (Fig. 4; Table 9). It should also be noted that Herculano-Houzel (2011) derived whole brain metabolism values by multiplying mass-specific rates reported in Karbowski (2007) by brain masses for her specimens. We also analyzed the data using the brain

Table 5
Bivariate regressions of arterial canal areas on endocranial volume (ECV). Each row is the output of one analysis. Note that for each clade sample or functional group, RSE is lowest, while adjusted r^2 and F are greatest when ACA is the response variable. Since a true ACA value would have to include the rete area for cheirogaleids, dermopterans and lorisiforms, and this value is not measureable from bony correlates, we did not include 'strepsirrhine' or 'rete' subgroups iterations of ACA ~ ECV.

Sample	ʎ	*n*	Intercept		Slope				RSE	Adj-r^2	F
			Mean (±SE)	CI	Mean (±SE)	CI	t	p			
lnDPA ~ lnECV											
Euarchonta	**0.99**	38	−2.16 (±0.37)	±0.75	0.78(±0.06)	±0.13	12	<0.0001	**0.77**	**0.80**	**147**
ICA + VA	0	26	−1.64 (±0.12)	±0.26	0.86 (±0.03)	±0.06	29	<0.0001	0.27	0.97	835
ECA + VA	1	11	−3.57 (±0.45)	±1.02	0.92 (±0.15)	±0.33	6	0.0002	0.71	0.79	39
VA-only	1	12	−3.65 (±0.42)	±0.94	0.80 (±0.11)	±0.23	8	<0.0001	0.53	0.84	58
lnDTFA ~ lnECV											
Euarchonta	**0.71**	38	−0.30 (±0.18)	±0.37	0.71(±0.04)	±0.08	17	<0.0001	**0.38**	**0.89**	**302**
ICA + VA	0	26	−0.38 (±0.12)	±0.24	0.68 (±0.03)	±0.06	24	<0.0001	0.25	0.96	597
ECA + VA	1	11	−0.39 (±0.34)	±0.77	0.78 (±0.11)	±0.25	7	<0.0001	0.54	0.83	49
VA-only	1	12	−0.29 (±0.28)	±0.63	0.79 (±0.07)	±0.16	11	<0.0001	0.35	0.92	127
lnACA ~ lnECV											
Euarchonta	**0.64**	38	−0.15 (±0.12)	±0.24	0.75 (±0.03)	±0.06	27	<0.0001	**0.25**	**0.95**	**742**
ICA + VA	0	26	−0.15 (±0.08)	±0.17	0.74 (±0.02)	±0.04	38	<0.0001	0.18	0.98	1444
VA-only	1.0	12	−0.25 (±0.28)	±0.62	0.80 (±0.07)	±0.15	11	<0.0001	0.34	0.92	132

Abbreviations: **Sample:** see SOM Table S5 for which taxa are included in each subset and Tables 3 and 5 for explanation of sample categories. **Variables:** See Table 3 for explanation of variables.

Table 6
Results of phylogenetic ANOVAs with post hoc comparisons. Note that differences, t and p are minimized using ACA residuals.

Data	ʎ	df	MS	VA-only vs. ICA + VA			ECA + VA vs. ICA + VA			VA-only vs. ECA + VA		
				Diff.	t	*p*	Diff.	t	*p*	Diff.	t	*p*
DPA res.	0.58	46	0.38	−2.12	9.16	<0.0001	−1.85	8.54	<0.0001	−0.27	1.74	0.08
DTFA res.	0	46	0.25	0.6	7.33	0.0001	0.15	1.89	0.065	0.44	4.5	<0.0001
ACA res.	0	46	0.21	0.18	2.68	0.01	−0.17	2.55	0.01	0.35	4.44	<0.0001

Comparisons of residuals of regression lines of ln(foramen cross-sectional area) vs. ln(endocranial volume) of sample "ANOVA" (see Table 1 and SOM Table S5 for data and sample taxa composition, respectively). Values in post-hoc cells are differences between mean values of the two groups compared (diff.), followed by the t-value and p-value of a student's t-test comparing the two groups. Abbreviations: MS, mean square error; df, degrees of freedom; ʎ, Pagel's lambda; ICA + VA = taxa with primarily brain blood supply from the internal carotid arteries and vertebral arteries; VA only = taxa with primary brain supply from the vertebral arteries; Rete = taxa with primary brain supply from the vertebral arteries and rete mirable.

Table 7
Multiple regression of carotid dominance (DPA/DTFA) on encephalization quotient (EQ), forebrain/hindbrain ratio (Fore/hind), and endocranial volume/body mass ratio (ECV/BM).

	Euarchonta	ICA + VA	VA Only
	$n = 26$, df = 22	$n = 19$, df = 15	$n = 7$, df = 3
Intercept			
Mean (±SE)	−3.24 (±1.78)	−2.60 (±1.78)	−2.58 (±3.14)
EQ coeff.			
Mean (±SE)	0.50 (±0.47)	0.77 (±0.46)	−1.16 (±1.32)
t Ratio	1.08	1.69	−0.87
p (mean = 0)	0.29	0.11	0.45
Fore/hind coeff.			
Mean (±SE)	0.85 (±0.81)	0.42 (±0.80)	3.59 (±2.85)
t Ratio	1.05	0.53	1.26
p (mean = 0)	0.30	0.60	0.30
ECV/BM coeff.			
Mean (±SE)	−0.08 (±0.34)	−0.26 (±0.33)	1.27 (±1.26)
t Ratio	−0.23	−0.77	1.00
p (mean = 0)	0.82	0.45	0.39
Overall stats			
λ	1.0 (ML)	1.0	1.0
Adjusted r^2	0.18	0.24	−0.28
F ratio	2.89	2.95	0.56

Abbreviations: **Sample:** See Table 3 for explanation of sample category and SOM Table S5 for taxa composition. **Variables:** EQ (encephalization quotient calculated from present sample), Fore/hind (natural log of forebrain to hind brain mass ratio from Stephan et al., 1981, see Table S6); ECV/BM (natural log of endocranial volume to body mass ratio); λ, Pagel's lambda – value representing phylogenetic signal of data; df, degrees of freedom; SE, standard error of estimate; p, probability of zero value of parameter; adjusted r^2, adjusted coefficient of determination for correlation; ML, maximum likelihood value of Pagel's lambda.

masses and BGU values reported by her (and by computing *Oryctolagus* BGU values via her method). The results are slightly different in that, while the model as a whole is highly significant, none of the independent variables is significant at $p < 0.05$. However, ACA has the highest t-value and lowest p value (suggesting it explains the most variance). By those criteria, ECV comes in second and neuron count still comes in third.

3.1. Predicting brain metabolic energy requirements using ACA

Given our interest in predicting brain metabolism in taxa for which soft tissue may not be available, we endeavored to construct a predictor of BGU using ACA and ECV but not neuron count. This approach is justified to some degree by the above findings that ACA and ECV consistently explain more variance in BGU than neuron count where data are available. We constructed our predictor utilizing a Bayesian approach that takes into account uncertainty in both phylogenetic signal and observed data (Nunn and Zhu, 2014). Jackknifing this approach shows an average prediction error of 6.7% relative to observed values of brain metabolism (SOM Table S7). It is notable that 6.7% error is still lower than the error rate associated with using neuron counts to predict brain metabolic energy consumption (7.8%) in a phylogenetically agnostic context (Herculano-Houzel, 2011). When we use ordinary least squares (a phylogenetically agnostic context) for predicting brain metabolism and use a jackknifing approach, our error rate is even lower (4.8%) (SOM Table S4).

Looking at BGU (as predicted by ACA and ECV) as a ratio of BMR,[4] we find that the 95% credibility limits on the value for *Homo sapiens* overlap with various other euarchontans. However, great apes, Old World monkeys, and gliroids have lower relative brain costs (Table 10; Fig. 5).

Table 8
Bivariate regressions of encephalization quotient (EQ), relative brain size and relative forebrain size on carotid dominance (DPA/DTFA). Pagel's lambda equals 1 in all analyses.

	Euarchonta	ICA + VA	VA only
EQ			
df (n−2)	34	24	10
F ratio	7.00	5.88	0.31
p (corr = 0)	0.01*	0.02*	0.59
ECV/BM			
df (n−2)	34	24	10
F ratio	4.24	0.03	0.24
p (corr = 0)	0.05*	0.86	0.64
Fore/hind			
df (n−2)	24	17	5
F ratio	6.43	7.66	0.80
p (corr = 0)	0.02*	0.01*	0.41

Abbreviations: **Sample:** See Table S5 for which taxa were included in each subset. **Variables:** EQ (encephalization quotient calculated from present sample), Fore/hind (natural log of forebrain to hind brain mass ratio from Stephan et al., 1981); ECV/BM (natural log of endocranial volume to body mass ratio); df, degrees of freedom; p, probability of no correlation. * denotes significant results.

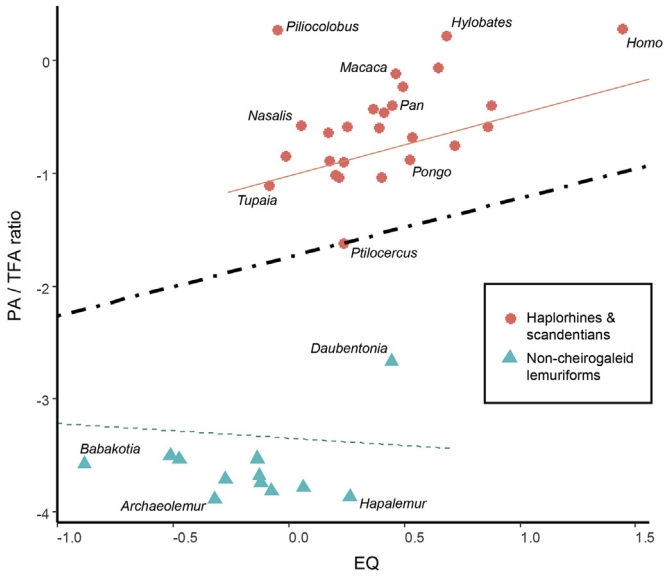

Figure 3. Ratios of the promontorial canal cross sectional area (PA)/transverse foramen cross sectional area (TFA) vs. encephalization quotient (EQ). EQ was measured as the difference in ln(ECV observed) and ln(ECV predicted) value of endocranial volume (ECV) given body mass (BM) using the equation lnECV = 0.76*ln BM − 2.56.

4. Discussion and conclusions

In the following discussion, we restate the major hypotheses as questions and explore the implications of our results.

4.1. Is variation in cerebrum blood demands reflected by carotid arteries alone?

We looked at this question in two ways, one where we asked whether variation in the transverse foramen cross-sectional area helps to explain variance in forebrain volume (Table 3), and another where we asked whether forebrain volume helps to explain variation in the cross-sectional areas of transverse foramina (Table 4).

[4] To make the comparison between brain metabolism and basal metabolic rate we had to convert μmol glucose/min into Kcal/day. To make this conversion, values in μmol glucose/min are multiplied by 0.988 to convert to Kcal/day.

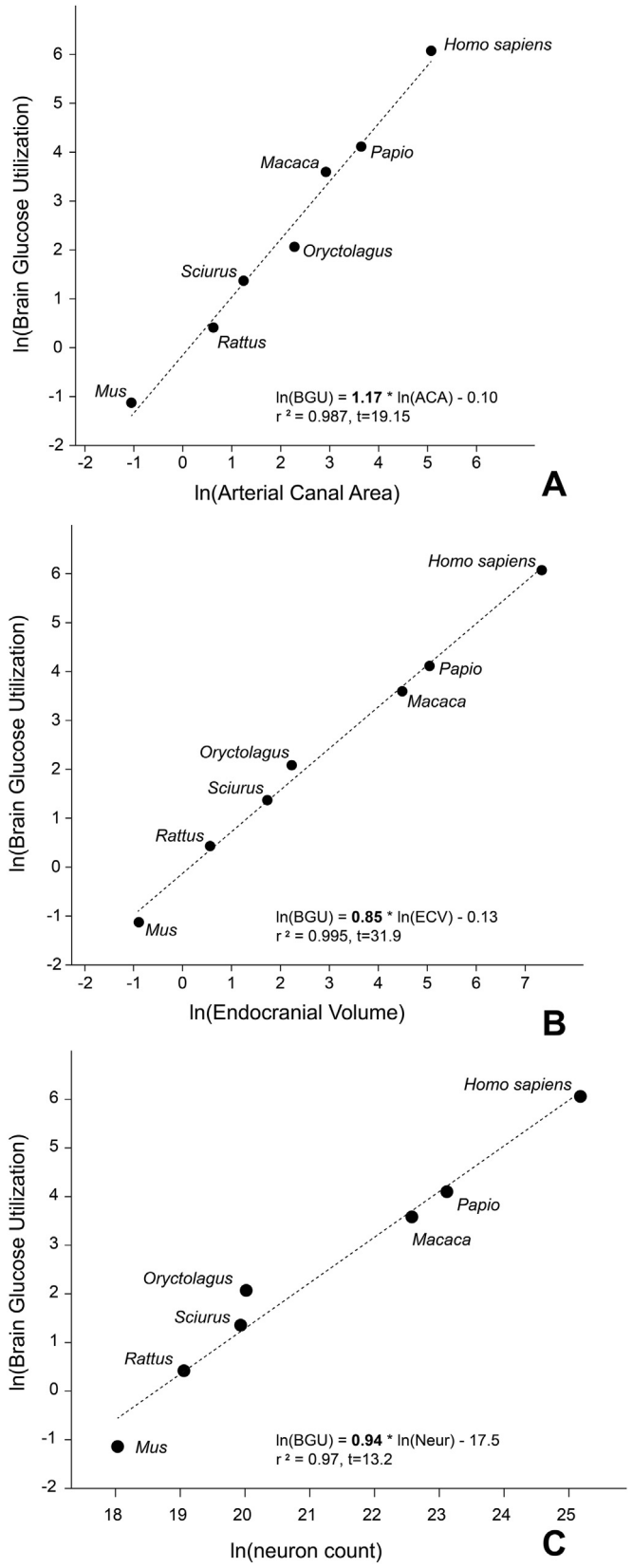

Figure 4. Correlation between Brain Glucose Utilization rates, brain mass and brain arterial canal diameters. All data are natural log transformed and each point represents a species mean value. **A**, Whole Brain Glucose Utilization (BGU) v. Total arterial cross sectional area (ACA). **B**, Whole Brain Glucose Utilization (BGU) v. Endocranial volume (ECV). **C**, Whole Brain Glucose Utilization (BGU) v. Neuron count. Utilizing both ACA and ECV in a multiple regression model for predicting BGU reveals both variables contribute independently to explaining variance and together explain more than 99.9% of variance. The predictor is extremely accurate according to leave-one-out approach, which averages only 4.7% error. Adding neuron counts to the set of predictor variables, does not, however, significantly improve the relationship (see also SOM Table S4).

Table 9
Multiple regression Brain Glucose Utilization rate from seven taxa in Table 2 on arterial canal area (ACA), endocranial volume (ECV) and neuron count (Neur).

Variable	Coeff. (±SE)	t	*p*	r^2
Intercept	3.88 (±2.35)	1.66	0.20	na
ln(ACA)	0.31 (±0.08)	3.73	0.03	0.987
ln(ECV)	0.82 (±0.17)	4.86	0.02	0.995
ln(Neur)	−0.22 (±0.13)	−1.71	**0.19**	0.972

In the first set of analyses, we found that transverse foramen cross-sectional areas always help to explain variance in forebrain size whether we looked at all euarchontans or particular 'functional groups'. In the second set, we found that variance in transverse foramen cross-sectional area is generally explained by variance in both forebrain volume and body mass. However, due to marginal significance, forebrain volume does not technically help explain variance in transverse foramen area in non-cheirogaleid lemuriforms. While this last result could suggest that the vertebral artery does not contribute meaningful amounts of blood to the forebrain in this group, that would appear to be impossible as lemurids and indriids have no alternative encephalic blood supply routes. It is more likely that this result reflects the limited power of the analysis, with only six taxa – all with similar brain size – available in the Stephan et al. (1981) dataset on brain structures.

We interpret these results to suggest that, while the vertebral artery is critical for supplying the forebrain with blood in all primates (and thus is bigger in species with bigger forebrains), the size of the transverse foramen is also influenced importantly by body mass, which can obscure the correlation with brain size in some cases. All things considered, these results suggest that predictions of cerebral blood flow and estimates of blood flow scaling that utilize the internal carotid canal alone (Seymour et al., 2015, 2016) could be misleading.

In the context of our study, it is worth noting that findings of previous research also question the idea that interspecific variation in cerebral blood flow can be adequately modeled without the vertebral artery. First, measures of blood flow in sheep and cows show that circle of Willis anastomoses allow the vertebral arteries to compensate for obstruction of the carotids (Baldwin and Bell, 1963). Furthermore, experiments using radioactively labeled microbeads injected into the vertebral arteries of cats and dogs recover a small radioactive signal in some cerebral structures (particularly in the occipital lobe), suggesting some vertebral-basilar artery contribution to cerebral circulation (Reneman et al., 1974; Wellens et al., 1975). In humans, the posterior cerebral artery appears to be a direct distributary of the basilar artery in 72% of adult humans (Krayenbühl et al., 1982) and is said to supply the caudal diencephalic structures (e.g., thalamus), the inferior temporal lobe, and the occipital lobe of the cerebral cortex (Tatu et al., 1998; White and Cant, 2016). Moreover, several studies using fMRI have quantified the rate of blood flow and mapped the vertebral-basilar arterial contribution to the posterior cerebrum (Hendrikse et al., 2004; Kansagra and Wong, 2008).

While van Bel et al. (1994) suggest carotid flow can be used to predict cerebral perfusion in sheep fetuses due to a strong correlation between these two variables, the relationship they recover is far from perfect or linear. Given our findings, we think that adding data on the vertebral arteries for those fetuses would likely have

Table 10
Brain Glucose Utilization predicted (pBGU) from ACA and ECV using phylogenetic prediction of Nunn and Zhou (2014) for all taxa where basal metabolic rate (BMR) is also available, and pBGU as a percentage of BMR. 95% CrI based on a posterior distribution of 99 predictions.

Taxon	BMR (Kcal/day)	Mean pBGU (Kcal/day)	95% CrI pBGU	(pBGU/BMR)%	95% CrI (pBGU/BMR)%
Rattus norvegicus	28.89	1.48	1.26–1.65	5.11	4.34–5.71
Mus musculus	4.6	0.32	0.28–0.37	6.93	6.07–8.00
Sciurus carolinensis	49.59	3.74	3.46–4.08	7.54	6.98–8.23
Oryctolagus cuniculus	159.81	7.51	6.15–9.11	4.70	3.85–5.70
Tupaia glis	10.78	1.88	1.52–2.29	17.41	14.11–21.21
Ptilocercus lowii	4.99	1.27	0.98–1.57	25.53	19.63–31.47
Propithecus sp.	86.8	16.27	13.09–19.34	18.74	15.08–22.28
Eulemur fulvus.	42	12.53	9.20–15.75	29.84	21.90–37.51
Lemur catta	45.1	13.34	9.80–16.46	29.57	21.72–36.50
Lepilemur sp.	27.6	5.24	4.22–6.46	18.98	15.28–23.39
Varecia sp.	69.9	16.57	13.24–20.95	23.71	18.94–29.97
Tarsius sp.	8.9	2.18	1.72–2.66	24.48	19.37–29.94
Callithrix jacchus	22.8	4.78	4.11–6.13	20.97	18.02–26.88
Cebuella pygmaea	10.1	2.82	1.99–3.37	27.93	19.71–33.37
Saimiri sciureus	68.8	12.43	10.90–15.06	18.06	15.85–21.89
Aotus trivirgatus	52.4	10.06	8.17–12.72	19.19	15.58–24.27
Alouatta sp.	231.9	29.15	23.57–36.49	12.57	10.16–15.73
Macaca fascicularis	251.01	35.75	30.08–40.29	14.24	11.99–16.05
Papio anubis	435.4	65.74	58.26–74.51	15.10	13.38–17.11
Pongo pygmaeus	1037	148.37	123.72–191.90	14.31	11.93–18.51
Pan troglodytes	1370	132.96	111.83–154.93	9.71	8.16–11.31
Homo sapiens	1557	420.55	338.66–489.80	27.01	21.75–31.46

Abbreviations: CrI, Bayesian credibility interval; Kcal/d, kilocalories per day. Data Sources*:* BMR for non-hominoids comes from McNab (2008) and Leonard et al. (2003). See Table 1 for taxon specific sources. BMR for *Pongo, Homo* and *Pan* comes from Pontzer et al. (2016) and represents species mean for sexes. BMR for *Mus* and *Oryctolagus* is the average of values from Kleiber (1947) and Tacutu et al. (2013). BMR for remaining gliroids comes from Tacutu et al. (2013).

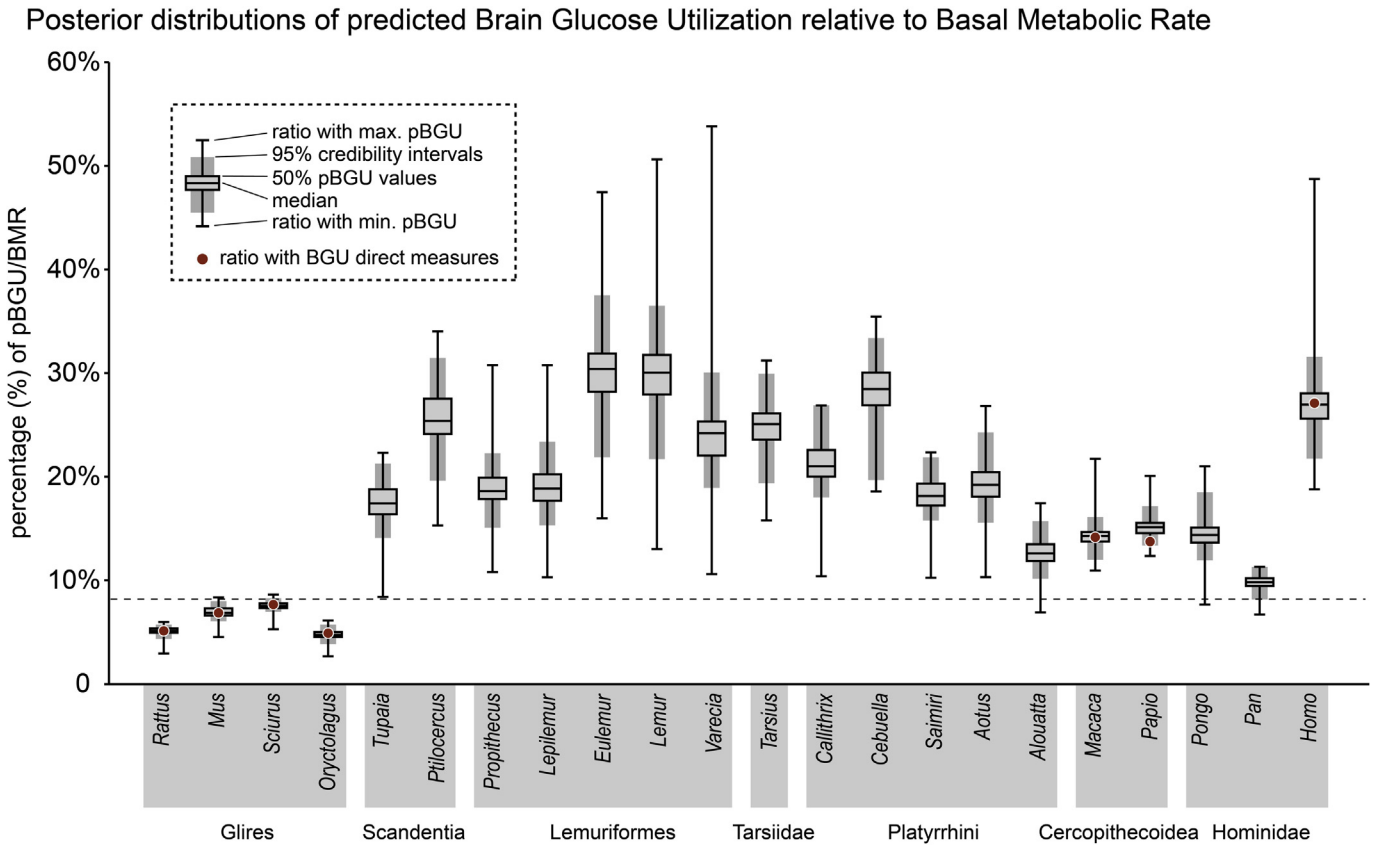

Figure 5. Percentage of Brain Glucose Utilization to whole body BMR. Brain Glucose Utilization (BGU) was predicted using total arterial canal area (ACA) and endocranial volume (ECV) with the Bayesian phylogenetic prediction routine of Nunn and Zhu (2014). Red dots indicate directly measured values in taxa used to generate the predictive equation. Note that all dots are within the 95% credibility intervals of the posterior distribution of predicted values. We also predicted each of the seven taxa with known BGU values from a subsample of the other six. The intervals for these taxa are plotted in SOM Figure S1. (For interpretation of the references to color in this figure legend, the reader is referred to the web version of this article.)

improved the correlations they observed. Finally, no study has assessed whether the relationship between measured (as opposed to predicted) carotid flow rates and cerebral blood perfusion varies interspecifically and whether such variation could be explained by taxon-specific differences in vertebral artery reliance.

4.2. Do strepsirrhine and non-strepsirrhine euarchontans get equivalent amounts of encephalic blood for a given brain size?

The idea that different primates may require different amounts of blood for a given brain size stems from studies estimating blood flow from the internal carotid artery alone (Seymour et al., 2015, 2016). As already discussed, Seymour et al. (2015) found that anthropoids have a greater exponent relating predicted blood flow rates through the internal carotid artery to brain size than do marsupials. While their data also show non-cheirogaleid lemuriforms to have a greater exponent than either haplorhines or marsupials, the internal carotid canal of non-cheirogaleid lemuriforms and other taxa with a stapedial artery is not functionally comparable to that of anthropoids and marsupials, which lack stapedial arteries. Although Seymour et al. (2015) acknowledge their data are problematic in this regard and that strepsirrhines supply the cerebrum without relying on the internal carotid artery, their discussion implies that haplorhines should have a higher slope and/or intercept relating forebrain blood flow to forebrain volume than strepsirrhines because they link increased scaling rates of blood flow to increased cognitive capacities, such as those involved in navigating complex social systems (Dunbar, 1998), which tend to be much less developed in strepsirrhines. (e.g., Sandel et al., 2011; Maille and Roeder, 2012).

Our results point toward the conclusion that strepsirrhine and non-strepsirrhine euarchontan brains require similar amounts of blood since phylogenetic ANCOVAs suggest haplorhines and non-cheirogaleid lemuriforms have an identical scaling relationship between ACA and ECV. Furthermore, the relationship between ACA and ECV among all euarchontans is tighter than that for either DPA vs. ECV or DTFA vs. ECV. In other words, there do not appear to be any clade offsets when looking at ACA against ECV, while the clade offsets are quite pronounced when looking at specific encephalic arteries. Not even humans deviate from the scaling relationships documented here, since human brain size is well-predicted by ACA.

More specifically, these findings predict that the vertebral artery must make up for a reduced/absent promontorial artery in non-cheirogaleids as compared to other strepsirrhines and haplorhines. Comparing relative size of arterial canals, our data support this prediction. We found that non-cheirogaleid lemuriforms have significantly higher residuals of transverse foramen area than do non-strepsirrhines with a large promontorial artery and strepsirrhines with an ascending pharyngeal artery. This supports the notion that there are three basic patterns of encephalic artery reliance among extant euarchontans (Conroy, 1982; MacPhee and Cartmill, 1986): 1) internal carotid reliance (treeshrews, tarsiers, and anthropoids), 2) external carotid ascending pharyngeal/rete mirable compensation for reduced internal carotid (cheirogaleids, lorisiforms, and dermopterans) and 3) vertebral artery reliance (non-cheirogaleid lemuriforms).

Although our results clearly demonstrate that ACA scaling is uniform among euarchontan groups, why certain groups of primates have a higher exponent relating promontorial canal area to brain size remains unanswered. Both Saban (1963, 1975) and Conroy (1982) suggest that a basic trend in primate evolution was the increasing dominance of the carotid over the vertebral system in brain irrigation. Saban (1963) devised a “carotid index” that quantified the relative size of the carotid foramen to the transverse foramen, and found that it increases in size as one looks from strepsirrhines to platyrrhines, to cercopithecoids, to apes, with humans having the relatively largest carotid foramina, a pattern corroborated by the current study. However, at least to our knowledge, Saban did not propose a hypothesis integrating and explaining these observations. Conroy (1982) suggested greater carotid dominance may reflect a larger forebrain. Though the strepsirrhine-like state (carotid-reduced) is probably not primitive (Boyer et al., 2016), there may still be some merit to the idea that carotid dominance increased over time in at least some clades of primates. If more encephalized species (like humans) tend to have greater carotid dominance, then carotid dominance may have increased over primate evolution along with documented increases in encephalization (Pagel, 2002; Gonzales et al., 2015; Harrington et al., 2016). Alternately, variation in carotid dominance could reflect variation in forebrain size relative to the hindbrain (Conroy, 1982).

According to our results, EQ and forebrain/hindbrain volume tend to have a stronger association with carotid dominance than does brain/body mass ratio (Fig. 3). While these relationships are not significant within non-cheirogaleid lemuriforms, this makes sense if the internal carotid artery is not relied upon by any non-cheirogaleid lemuriforms regardless of relative brain size. It is, however, intriguing that the most encephalized strepsirrhine, *Daubentonia*, also has the absolutely largest promontorial canal and greatest degree of carotid dominance among strepsirrhines. If *Daubentonia*'s larger promontorial canal actually reflects carotid dominance, then it should contain a patent promontorial artery, but this region of *Daubentonia*'s soft anatomy has never been examined, to our knowledge.

To us, these results suggests that evolutionarily, when a lineage's brain size increases ‘faster’ than its body size, the disproportionate increase in the brain's blood demands will be met more readily by expansion of the promontorial artery than by the vertebral artery. If the internal carotid enlarges relative to the vertebral artery because the brain is getting bigger relative to body size, the corollary is that the vertebral artery is tracking body size more closely. This idea is consistent with our finding that both brain mass and body mass help explain variation in transverse foramen size (as discussed above), while only brain size explains variation in the promontorial canal (Boyer et al., 2016).

The relationship between carotid dominance and encephalization may also explain the finding by Seymour et al. (2016) that cerebral blood flow scales with brain size to the 1.41 power in hominins. This exponent implies that as hominin brains increased in absolute and relative size, their mass-specific tissue demands also increased, compounding the total expense to their owners. The authors specifically claim that while brain size increased by 3.5 times in human evolution, brain cost increased by six times. Even before we conducted this study, it should be noted that one of the predictions of the Seymour et al. (2016) study (that tissue- or neuron-specific costs of human brain tissue should be greater than for other animals) does not appear to hold (Karbowski, 2007; Herculano-Houzel, 2011).

Given this prior evidence that tissue specific metabolic demands of the human brain are not exceptional and our findings that taxa with higher EQ's have greater carotid dominance, we prefer an alternate explanation of hominin carotid scaling: we suspect that Seymour et al.'s (2016) exponent of 1.41 reflects increasing internal carotid dominance with increasing EQ during Plio-Pleistocene hominin evolution. If data on transverse foramen diameters were available for the fossil hominins they analyzed, we expect that the exponent of the relationship between total encephalic arterial canal area (ACA) and brain size would be close to what was measured for other euarchontan groups here. If not – that is, if hominins are

found to exhibit a greater slope of ACA to ECV than other primates and mammals—this would support Seymour et al.'s (2016) hypothesis. Thus, recovery of associated cervical vertebrae for fossil hominins is an important goal.

4.3. Does total encephalic arterial flow reflect brain metabolic demands?

As discussed above, it seems that blood flow rates should track metabolic energy consumption. Unfortunately, the potential for obtaining reliable predictions of blood flow based on arterial canal diameters remains low (SOM S1). Furthermore, other authors have noted reasons why even reliable measures of flow might not reflect metabolic energy use. We avoid many (but not all) of the problems associated with estimating flow from canal measures by using measures of arterial canal size to directly model variation in brain metabolic costs.

Our approach to this question was to check whether variation in ACA helps to explain variation in BGU in the context of other variables thought to explain a large amount of metabolic variance. We found that ACA explains significant amounts of variation in BGU along with brain size, whereas neuron counts do not. We interpret this to mean that there are more nuisance parameters relating BGU to neurons than to ACA and ECV. For instance, the study of Herculano-Houzel (2011) shows that average mass specific costs of cerebellar tissue are quite close to those of cerebral tissue even though cerebral neurons cost much more than cerebellar neurons. To us, this suggests 1) that more than just neuron number is determining energy consumption, and 2) structure mass helps capture these effects.

More importantly, our results suggest that BGU predictions based on ECV and ACA will be more reliable than those based on neuron counts alone. In fact, comparing the prediction error in BGU using neuron counts to that using ACA and ECV shows that the available neuron count data yield a greater percentage prediction error. This is fortuitous, since it means BGU can be computed for fossil taxa where neuron counts will never be available.

Of course, we acknowledge that additional data representing direct measures of brain metabolism and neuron counts for more species could change these conclusions. It would be particularly important to get direct measures of brain metabolism for gliroids and primates with similar brain sizes, but dramatically different neuron numbers. For instance, *Callithrix jacchus* has a brain of similar size to that of *Oryctolagus*, but with 1.3 times the number of neurons (Herculano-Houzel et al., 2015). Likewise, the agouti (*Dasyprocta prymnolopha*, a rodent) and owl monkey (*Aotus trivirgatus*) have similarly sized brains, but the agouti has about half the number of neurons. If neuronal numbers are as important as previously suggested, these additional data should tip the scales away from brain size and towards neuron counts for explaining brain metabolism.

4.4. What do arterial canals suggest about variation in brain metabolic energy requirements?

Having made the case that 1) there is a relatively uniform relationship between ECV and ACA among euarchontans, and 2) that ACA and ECV can predict BGU relatively well without knowledge of neuronal properties, we tentatively explore some implications of predicting BGU in taxa for which these values cannot be directly measured.

First, we note that looking at predicted brain metabolic demands (pBGU) as a percentage of basal metabolic rate (BMR) supports previous studies using actual BGU (Armstrong, 1985) by suggesting that humans have a higher relative brain cost than gliroids and cercopithecoids (Fig. 5). Our findings also support the intuitive assumption that other hominids (*Pan* and *Pongo*) should have a brain cost that is relatively lower than in humans (Aiello and Wheeler, 1995; Pontzer et al., 2016). The surprise comes when looking at relative brain cost of certain treeshrews, lemurs, tarsiers and platyrrhines. What is surprising is that they are predicted to be essentially human-like in their relative brain cost (Fig. 5). However, these depictions of relative brain cost should be seen as tentative, as measurements of only seven species were available for generating the predictions of brain metabolic demands (Table 3).

Considering the tentative nature of these predictions, the reader may find the apparent heterogeneity in 95% credibility intervals among taxa in Figure 5 concerning. That is, taxa with smaller average predictions of relative brain cost appear to have tighter credibility intervals, while those with larger average predictions that are close to humans values tend to have wider intervals. Does this mean we should be particularly skeptical of the predictions overlapping human values? We think not. These apparent differences in interval width are mostly an artifact of plotting method. For the purpose of presenting an intuitive y-axis scale, we chose to plot data of Figure 5 with arithmetic units (percentage of pBGU relative to BMR) even though the variation in the data necessarily follows a log-normal distribution. Nonetheless, even in log-space there is still a trend between the size of the credibility interval and the mean value of pBGU/BMR. However, the trend is very slight with the widest interval only 1.6 times the smallest interval for a taxon without direct BGU measures. Furthermore, there is a lot of scatter in the trend. As an example of scatter, tarsiers, *Lepilemur, Pongo* and *Alouatta* have log-credibility intervals of identical width, but only tarsiers have an upper 95% credibility interval ratio that overlaps with the mean human pBGU/BMR value. Furthermore, we show that using predictors based on only six taxa greatly increases the width of the credibility intervals for gliroids of our sample, but does not affect the accuracy of the mean pBGU values for those species (SOM Table S7; Fig. S1). Therefore, larger credibility intervals do not appear indicative of predictor failure.

Reconsidering the possibility that neuron counts would provide a better assessment of brain cost, let us examine *Oryctolagus* again. This taxon has a measured BGU of 7.93 μmol/min (Passero et al., 1981). The fact that *Oryctolagus* has less than three-quarters the number of neurons found in *C. jacchus* would suggest it has a lower total brain metabolism compared to *C. jacchus*. While actual BGU is not available for *C. jacchus*, we can still learn something interesting by looking at predicted values.

Using the neuron count regression from Herculano-Houzel (2011) predicts a much lower metabolic rate for the brain of *Oryctolagus* at ~2 μmol/min. This is necessarily lower than the value predicted for *C. jacchus* (3.68 μmol/min), given the monkey's greater neuron count. However, note the large discrepancy between measured (7.93 μmol/min) and predicted (~2 μmol/min) brain metabolism values for *Oryctolagus* when using neurons. In contrast, when using ACA and ECV as predictors, *Oryctolagus* is predicted at 7.13 μmol/min based on six other taxa with measured BGU, which is very close to the measured value. The prediction for *C. jacchus* does not change as much using the ACA + ECV proxy (4.8 μmol/min). Therefore, this comparison suggests 1) that ACA + ECV predicts brain metabolism in *Oryctolagus* more accurately than does neuron number, and 2) that *Oryctolagus* has a higher brain metabolism than *C. jacchus*, despite having fewer neurons.

While it is possible that the available brain metabolism measurement of *Oryctolagus* is inaccurate, we can assess the relative plausibility of the measured versus neuron-predicted values by looking at the ratio of pBGU/BMR. If the neuron-predicted value of ~2 μmol/min is used, this puts *Oryctolagus* in a class by itself with

very low relative brain costs at ~1.2% of its BMR, whereas the actual value (7.93 μmol/min) and that predicted by ACA and ECV (7.13 μmol/min) makes it similar to other gliroids with a value of ~5% (Fig. 5, Table 10). Again, additional data representing direct measures of brain metabolism are important for moving the field forward.

If some euarchontans have relative brain costs that approach or surpass those of humans, then the human brain cannot be considered exceptionally expensive and there are some interesting implications. Management of relatively high brain costs and risks associated with brain malnourishment may not be enough to explain many novel aspects of hominin origins or even the elevated human daily total energy expenditure (TEE) (Pontzer et al., 2016). It is possible that other hominin traits have independently driven up TEE and selected for enhanced cognitive processes. One example implication here is that human adiposity may not be a trait for buffering the brain per se, because other euarchontans with brains that are similarly expensive (according to our results) do not display such adiposity (Navarrete et al., 2011). Instead, adiposity seems more likely to be a buffer against an energy budget that is high for a variety of reasons (e.g., needing to manage costs of simultaneously permitting a large daily foraging range, longevity, and high reproductive rates) in a feast/famine context (Kaplan et al., 2000). In this context, it is still possible that high levels of adult adiposity (relative to human juveniles and adults of other species) are an indirect response to large brains in the sense that stores of body fat may serve as a buffer for adults who, at times, sacrifice their own nourishment in order to provision the developing brains of their offspring. This would explain why brain energetic demands do not correlate with average levels of adiposity during human ontogeny (Kuzawa et al., 2014).

Also intriguing is the finding that euarchontans may devote greater energy to their brains relative to BMR than do non-euarchontans sampled here. It upholds and expands Armstrong's (1983, 1985) similar perspective about primates with more data. One may question whether this reflects a lower-than-expected BMR for body size among euarchontans. Other studies show that this is not the case, as primates are typical of most mammals in the relationship they express between body size and BMR (McNab, 2008; Weisbecker and Goswami, 2010; Pontzer et al., 2014). On the other hand, primates tend to have depressed daily TEE (Pontzer et al., 2014) for their body size. Using TEE in place of BMR in this study would only accentuate the gap between euarchontans and other mammals.

So what explains a higher relative brain cost in euarchontans? For the current sample, these differences can probably mostly be explained by gliroids having a smaller brain size and arterial canal size relative to body size than the euarchontans. These differences also correspond to greater neuron counts relative to body size in the euarchontans, and therefore, potentially greater cognitive complexity.

Our findings raise the possibility that the capacity for growing a larger, more metabolically expensive brain evolved in the ancestral euarchontan lineage and distinguished it from its gliroid sister lineage. This capacity may have been enabled by life history changes such as decreased litter size and increased gestation lengths, which also tend to distinguish euarchontans from gliroids today (Pagel and Harvey, 1988; Weisbecker and Goswami, 2010). Whether the ability to grow a relatively more expensive brain happened accidentally and predisposed euarchontan descendent lineages to selection for increased cognitive complexity, or whether selection for greater cognitive complexity resulted in adaptive changes for sustaining a more expensive brain is not addressed by our study.

5. Summary

This study investigated the patterns of variation in the cross sectional area of the transverse foramina of the cervical vertebrae to ask whether the vertebral artery contributes to cerebral blood supply in an important way. We also explored the tentative implications of our data for evolutionary variation in brain metabolism. Our sample included 49 euarchontan and four gliroid taxa representing 287 individuals. For some analyses, we coupled the data from the transverse foramina with data from the promontorial canal of the internal carotid artery from a previous study. Our analyses lead to the following conclusions:

1) The vertebral artery contributes significantly to both cerebral and cerebellar blood flow in all euarchontans.
2) Cognitive differences between major primate groups (haplorhines and strepsirrhines) do not affect the relationship between total encephalic arterial canal size and brain size. A constant total canal area is maintained in different ways in different groups. Non-cheirogaleid lemuriforms have larger cervical transverse foramina for a given brain size, while non-strepsirrhine primates and treeshrews have a larger promontorial canal.
3) Variation in carotid dominance (ratio of promontorial canal area to transverse foramen area) is correlated with encephalization and relative forebrain size across Euarchonta and within haplorrhines. This relationship extends to *Daubentonia* among strepsirrhines. It suggests that evolutionary increases in brain size that are not accompanied by increases in body size are accommodated primarily by increasing the internal carotid artery size/capacity. This relationship suggests that during hominin evolution, the internal carotid arterial canal became disproportionately large relative to brain size because brain size was increasing relative to body size, not because hominin brain tissue was becoming more expensive.
4) Measurements of total encephalic arterial canal area are perhaps the best available proxy for brain glucose utilization rates based on a stronger statistical correlation with brain metabolism than neuron counts and sometimes brain size.
5) Using a Bayesian approach to predicting brain metabolism from arterial canal area and brain size suggests that the human brain is more expensive (relative to basal metabolic rate) than the brains of apes, cercopithecoids, and gliroids, but no more expensive than the brains of various other euarchontans, including tarsiers, as well as certain treeshrews, lemurs, and New World monkeys. Thus, while *Homo sapiens* appears to have evolved a more expensive brain since divergence from its common ancestor with chimpanzees, the ancestral euarchontan also appears to have evolved a more expensive brain after divergence from its common ancestor with Glires.
6) More remains to be learned regarding patterns of blood flow to the brain and the fidelity with which arterial canal diameter measurements can track them. Some important objectives for future research include obtaining direct measures of brain metabolism for additional primate and gliroid species, gross dissection and perfusion of cadavers to empirically determine available blood routes, and extending the present study to include measurements of the transverse foramina and carotid canals in marsupials, fossil hominins, and more gliroids.

Author contributions

DMB & ARH contributed equally to all aspects of the manuscript.

Acknowledgements

We thank the curators and staff at the American Museum of Natural History (N. Simmons, N. Duncan, R. Voss, E. Westwig, and B. O'Toole), the Smithsonian Institution's National Museum of Natural History (K. Helgen, and D. Lunde), and at the Duke Fossil Primate Center (G. Gunnell and C. Riddle) for graciously allowing us to use the collections space and take caliper measurements of specimens under their stewardship. We also thank the founders and managers of the KUPRI web site. Research was funded by NSF SBE-1028505 (to E.J. Sargis and S.G.B. Chester), Leakey Foundation Research Grant (to S.G.B. Chester), NSF BCS 1440742 (to D.M. Boyer and G.F. Gunnell), BCS 1440558 (to J. I. Bloch), BCS 1552848 (to D.M. Boyer), and DBI 1701714 (to D. Blackburn, E. Stanley, J. I. Bloch, and D. M. Boyer). Finally, we thank B. Hare, S. Alberts, S. Patek, C. Wall, G. Yapuncich, and S. Churchill for helpful comments/discussion on the development of this research. We thank C. Nunn and I. Miller for help with BayesModelS and comments on the manuscript. We thank four anonymous reviewers and the editors of Journal of Human Evolution for helpful evaluation of earlier versions of this manuscript.

Supplementary Online Material

Supplementary online material related to this article can be found at http://dx.doi.org/10.1016/j.jhevol.2017.09.003.

References

Abdi, H., 2007. Bonferroni and Šidák corrections for multiple comparisons. In: Neil, J., Salkind, N.J. (Eds.), Encyclopedia of Measurement and Statistics, Vol. 3. Sage Publications Inc, Thousand Oaks, CA and London, pp. 103–107.
Aiello, L.C., Wheeler, P., 1995. The expensive tissue hypothesis: the brain and the digestive system in human and primate evolution. Curr. Anthropol. 36, 199–221.
Armstrong, E., 1983. Relative brain size and metabolism in mammals. Science 220, 1302–1304.
Armstrong, E., 1985. Allometric considerations of the adult mammalian brain, with special emphasis on primates. In: Jungers, W.L. (Ed.), Size and Scaling in Primate Biology. Plenum Press, New York, pp. 115–146.
Baldwin, B.A., Bell, F.R., 1963. Blood flow in the carotid and vertebral arteries of the sheep and calf. J. Physiol. 167, 448–462.
Bauernfeind, A.L., Barks, S.K., Duka, T., Grossman, L.I., Hof, P.R., Sherwood, C.C., 2014. Aerobic glycolysis in the primate brain: reconsidering the implications for growth and maintenance. Brain Struct. Funct. 219, 1149–1167.
Bouilleret, V., Boyet, S., Marescaux, C., Nehlig, A., 2000. Mapping of the progressive metabolic changes occurring during the development of hippocampal sclerosis in a model of mesial temporal lobe epilepsy. Brain Res. 852, 255–262.
Boyer, D.M., Kirk, E.C., Silcox, M.T., Gunnell, G.F., Gilbert, C.C., Yapuncich, G.S., Allen, K.L., Welch, E., Bloch, J.I., Gonzales, L.A., Kay, R.F., Seiffert, E.R., 2016. Internal carotid arterial canal size and scaling in Euarchonta: Re-assessing implications for arterial patency and phylogenetic relationships in early fossil primates. J. Hum. Evol. 97, 123–144.
Bugge, J., 1974. The cephalic arterial system in insectivores, primates, rodents, and lagomorphs, with special reference to the systematic classification. Acta Anat. 87, 1–160.
Cartmill, M., 1975. Strepsirhine basicranial structures and the affinities of the Cheirogaleidae. In: Luckett, W.P., Szalay, F.S. (Eds.), Phylogeny of the Primates: A Multidisciplinary Approach. Plenum Press, New York, pp. 313–354.
Cartmill, M., MacPhee, R.D.E., 1980. Tupaiid affinities: the evidence of the carotid arteries and cranial skeleton. In: Luckett, W.P. (Ed.), Comparative Biology and Evolutionary Relationships of Tree Shrews. Plenum Press, New York, pp. 95–132.
Changizi, M.A., 2001. Principles underlying mammalian neocortical scaling. Biol. Cybern. 84, 207–215.
Clarke, D., Sokoloff, L., 1994. Circulation and energy metabolism of the brain. In: Siegel, G., Agranoff, B., Alberts, R., Molinoff, P. (Eds.), Basic Neurochemistry. Raven Press, New York, pp. 645–680.
Coceani, F., Gloor, P., 1966. The distribution of the internal carotid circulation in the brain of the macaque monkey (*Macaca mulatta*). J. Comp. Neurol. 128, 419–429.
Conroy, G.C., 1982. A study of cerebral vascular evolution in primates. In: Armstrong, E., Falk, D. (Eds.), Primate Brain Evolution. Plenum Press, New York, pp. 247–261.
Conroy, G.C., Wible, J.R., 1978. Middle ear morphology of *Lemur variegatus*: Some implications for primate paleontology. Folia Primatol. 29, 81–85.
Deaner, R.O., Isler, K., Burkart, J., Van Schaik, C., 2007. Overall brain size, and not encephalization quotient, best predicts cognitive ability across non-human primates. Brain Behav. Evol. 70, 115–124.
Dunbar, R., 1998. The social brain hypothesis. Brain 9, 178–190.
Finarelli, J.A., Flynn, J.J., 2007. The evolution of encephalization in caniform carnivorans. Evolution 61, 1758–1772.
Fonseca-Azevedo, K., Herculano-Houzel, S., 2012. Metabolic constraint imposes tradeoff between body size and number of brain neurons in human evolution. Proc. Natl. Acad. Sci. 109, 18571–18576.
Frerichs, K.U., Dienel, G.A., Cruz, N.F., Sokoloff, L., Hallenbeck, J.M., 1995. Rates of glucose utilization in brain of active and hibernating ground squirrels. Am. J. Physiol. – Reg. I. 268, R445–R453.
Gonzales, L.A., Benefit, B.R., McCrossin, M.L., Spoor, F., 2015. Cerebral complexity preceded enlarged brain size and reduced olfactory bulbs in Old World monkeys. Nat. Commun. 67580, 1–6.
Grabowski, M., 2016. Bigger brains led to bigger bodies?: The correlated evolution of human brain and body size. Curr. Anthropol. 57, 174–196.
Grabowski, M., Voje, K.L., Hansen, T.F., 2016. Evolutionary modeling and correcting for observation error support a 3/5 brain-body allometry for primates. J. Hum. Evol. 94, 106–116.
Harrington, A.R., Silcox, M.T., Yapuncich, G.S., Boyer, D.M., Bloch, J.I., 2016. First virtual endocasts of adapiform primates. J. Hum. Evol. 99, 52–78.
Hawkins, R.A., Mans, A.M., Davis, D.W., Hibbard, L.S., Lu, D.M., 1983. Glucose availability to individual cerebral structures is correlated to glucose metabolism. J. Neurochem. 40, 1013–1018.
Hendrikse, J., van der Grond, J., Lu, H., Van Zijl, P.C., Golay, X., 2004. Flow territory mapping of the cerebral arteries with regional perfusion MRI. Stroke 35, 882–887.
Herculano-Houzel, S., 2011. Scaling of brain metabolism with a fixed energy budget per neuron: implications for neuronal activity, plasticity and evolution. PLoS ONE 6, e17514.
Herculano-Houzel, S., Collins, C.E., Wong, P., Kaas, J.H., 2007. Cellular scaling rules for primate brains. Proc. Natl. Acad. Sci. 104, 3562–3567.
Herculano-Houzel, S., Kaas, J.H., 2011. Gorilla and orangutan brains conform to the primate cellular scaling rules: implications for human evolution. Brain Behav. Evol. 77, 33–44.
Herculano-Houzel, S., Ribeiro, P., Campos, L., Valotta da Silva, A., Torres, L.B., Catania, K.C., Kaas, J.H., 2011. Updated neuronal scaling rules for the brains of glires (Rodents/Lagomorphs). Brain Behav. Evol. 78, 302–314.
Herculano-Houzel, S., Catania, K., Manger, P.R., Kaas, J.H., 2015. Mammalian brains are made of these: a dataset of the numbers and densities of neuronal and nonneuronal cells in the brain of glires, primates, scandentia, eulipotyphlans, afrotherians and artiodactyls, and their relationship with body mass. Brain Behav. Evol. 86, 145–163.
Hofman, M.A., 2014. Evolution of the human brain: when bigger is better. Front. Neuroanat. 8, 15.
Isler, K., 2013. Brain size evolution: how fish pay for being smart. Curr. Biol. 23, R63–R65.
Isler, K., van Schaik, C.P., 2006. Metabolic costs of brain size evolution. Biol. Lett. 2, 557–560.
Isler, K., Kirk, E.C., Miller, J.M., Albrecht, G.A., Gelvin, B.R., Martin, R.D., 2008. Endocranial volumes of primate species: scaling analyses using a comprehensive and reliable data set. J. Hum. Evol. 55, 967–968.
Jerison, H.J., 1955. Brain to body ratios and the evolution of intelligence. Science 121, 447–449.
Jerison, H.J., 1973. Evolution of the Brain and Intelligence. Academic Press, New York.
Kansagra, A.P., Wong, E.C., 2008. Mapping of vertebral artery perfusion territories using arterial spin labeling MRI. J. Magn. Reson. Imaging 28, 762–766.
Kaplan, H., Hill, K., Lancaster, J., Hurtado, A.M., 2000. A theory of human life history evolution: diet, intelligence, and longevity. Evol. Anthropol. 9, 156–185.
Karbowski, J., 2007. Global and regional brain metabolic scaling and its functional consequences. BMC Biol. 5, 1.
Karbowski, J., 2011. Scaling of brain metabolism and blood flow in relation to capillary and neural scaling. PLoS ONE 6, e26709.
Kennedy, C., Sakurada, O., Shinohara, M., Jehle, J., Sokoloff, L., 1978. Local cerebral glucose utilization in the normal conscious macaque monkey. Ann. Neurol. 4, 293–301.
Kleiber, M., 1947. Body size and metabolic rate. Physiol. Rev. 27, 511–541.
Krayenbühl, H., Yaşargil, M.G., Huber, P., 1982. Cerebral Angiography, 2nd ed. Thieme-Verlag, Stuttgart.
Krupenye, C., Kano, F., Hirata, S., Call, J., Tomasello, M., 2016. Great apes anticipate that other individuals will act according to false beliefs. Science 354, 110–114.
Kuzawa, C.W., Chugani, H.T., Grossman, L.I., Lipovich, L., Muzik, O., Hof, P.R., Wildman, D.E., Sherwood, C.C., Leonard, W.R., Lange, N., 2014. Metabolic costs and evolutionary implications of human brain development. Proc. Natl. Acad. Sci. 111, 13010–13015.
Leonard, W.R., Robertson, M.L., Snodgrass, J.J., Kuzawa, C.W., 2003. Metabolic correlates of hominid brain evolution. Comp. Biochem. Phys. A 136, 5–15.
Levant, B., Pazdernik, T.L., 2004. Differential effects of ibogaine on local cerebral glucose utilization in drug-naive and morphine-dependent rats. Brain Res. 1003, 159–167.
Lou, H.C., Edvinsson, L., MacKenzie, E.T., 1987. The concept of coupling blood flow to brain function: revision required? Ann. Neurol. 22, 289–297.

MacLean, E.L., 2016. Unraveling the evolution of uniquely human cognition. Proc. Natl. Acad. Sci. 113, 6348–6354.
MacPhee, R.D.E., 1981. Auditory Regions of Primates and Eutherian Insectivores: Morphology, Ontogeny, and Character Analysis. S. Karger, New York.
MacPhee, R.D.E., Cartmill, M., 1986. Basicranial structures and primate systematics. In: Swisher, D.R., Erwin, J. (Eds.), Comparative Primate Biology: Systematics, Evolution, and Anatomy. Alan R. Liss, New York, pp. 219–275.
Magistretti, P.J., Allaman, I., 2015. A cellular perspective on brain energy metabolism and functional imaging. Neuron. 86, 883–901.
Maille, A., Roeder, J.J., 2012. Inferences about the location of food in lemurs (*Eulemur macaco* and *Eulemur fulvus*): a comparison with apes and monkeys. Anim. Cogn. 15, 1075–1083.
Martin, R.D., 1981. Relative brain size and basal metabolic rate in terrestrial vertebrates. Nature 293, 57–60.
McNab, B.K., 2008. An analysis of the factors that influence the level and scaling of mammalian BMR. Comp. Biochem. Phys. A 151, 5–28.
Meguro, K., Blaizot, X., Kondoh, Y., Le Mestric, C., Baron, J., Chavoix, C., 1999. Neocortical and hippocampal glucose hypometabolism following neurotoxic lesions of the entorhinal and perirhinal cortices in the non-human primate as shown by PET. Brain 122, 1519–1531.
Münkemüller, T., Lavergne, S., Bzeznik, B., Dray, S., Jombart, T., Schiffers, K., Thuiller, W., 2012. How to measure and test phylogenetic signal. Methods Ecol. Evol. 3, 743–756.
Navarrete, A., van Schaik, C.P., Isler, K., 2011. Energetics and the evolution of human brain size. Nature 480, 91–93.
Nehlig, A., Boyet, S., 2000. Dose–response study of caffeine effects on cerebral functional activity with a specific focus on dependence. Brain Res. 858, 71–77.
Nehlig, A., de Vasconcelos, A.P., Boyet, S., 1988. Quantitative autoradiographic measurement of local cerebral glucose utilization in freely moving rats during postnatal development. J. Neurosci. 8, 2321–2333.
Nunn, C.L., Zhu, L., 2014. Phylogenetic prediction to identify "evolutionary singularities". In: Garamszegi, L.Z. (Ed.), Modern Phylogenetic Comparative Methods and Their Application in Evolutionary Biology. Springer-Verlag, Berlin, Heidelberg, pp. 481–514.
O'brien, R.M., 2007. A caution regarding rules of thumb for variance inflation factors. Qual. Quant. 41, 673–690.
Orme, C.D.L., Freckleton, R.P., Thomas, G., Petzoldt, T., Fritz, S.A., Isaac, N., Pearse, W., 2011. Caper: Comparative Analyses of Phylogenetics and Evolution in R. Available at. http://R-Forge.R-project.org/projects/caper/.
Pagel, M., Meade, A., 2013. BayesTraits v2. Distributed in author's web cite: http://www.evolution.rdg.ac.uk/Files/BayesTraitsV2Manual%28Beta%29.pdf (accessed 10.25.17).
Pagel, M.D., 2002. Modelling the evolution of continuously varying characters on phylogenetic trees. In: MacLeod, N., Forey, P.L. (Eds.), Morphology, Shape and Phylogeny. Taylor and Francis, London, pp. 269–286.
Pagel, M.D., Harvey, P., 1988. How mammals produce large-brained offspring. Evolution 42, 948–957.
Passero, S., Carli, G., Battistini, N., 1981. Depression of cerebral glucose utilization during animal hypnosis in the rabbit. Neurosci. Lett. 21, 345–349.
Pontzer, H., Brown, M.H., Raichlen, D.A., Dunsworth, H., Hare, B., Walker, K., Luke, A., Dugas, L.R., Durazo-Arvizu, R., Schoeller, D., Plange-Rhule, J., Bovet, P., Forrester, T.E., Lambert, E.V., Thompson, M.E., Shumaker, R.W., Ross, S.R., 2016. Metabolic acceleration and the evolution of human brain size and life history. Nature 533, 390–392.
Pontzer, H., Raichlen, D.A., Gordon, A.D., Schroepfer-Walker, K.K., Hare, B., O'Neill, M.C., Muldoon, K.M., Dunsworth, H.M., Wood, B.M., Isler, K., Burkart, J., Irwin, M., Shumaker, R.W., Lonsdorf, E.V., Ross, S.R., 2014. Primate energy expenditure and life history. Proc. Natl. Acad. Sci. 111, 1433–1437.
Reneman, R., Wellens, D., Jageneau, A., Stynen, L., 1974. Vertebral and carotid blood distribution in the brain of the dog and the cat. Cardiovasc. Res. 8, 65–72.
Saban, R., 1963. Contribution a l'etude de l'os temporal des primates. Description chez l'homme et les prosimiens. Anatomie comparee et phylogenie. Memo. Mus. Natl. d'Hist. Nat., Paris 1–368. Series A.
Saban, R., 1975. Structure of the ear region in living and subfossil lemurs. In: Tattersall, I., Sussman, R.W. (Eds.), Lemur Biology. Plenum Press, New York, pp. 83–109.
Sandel, A.A., MacLean, E.L., Hare, B., 2011. Evidence from four lemur species that ringtailed lemur social cognition converges with that of haplorhine primates. Anim. Behav. 81, 925–931.
Scheel, P., Ruge, C., Schoning, M., 2000. Flow velocity and flow volume measurements in the external carotid and vertebral arteries in healthy adults: reference data and effects of age. Ultrasound Med. Biol. 26, 1261–1266.
Schmidt-Nielsen, K., 1984. Scaling – Why is Animal Size so Important? Cambridge University Press, Cambridge.
Schöning, M., Walter, J., Scheel, P., 1994. Estimation of cerebral blood flow through color duplex sonography of the carotid and vertebral arteries in healthy adults. Stroke 25, 17–22.
Scremin, O.U., 2011. Cerebral vascular system. In: Mai, J., Paxinos, G. (Eds.), The Human Nervous System. Elsevier Academic Press, Amsterdam, Boston, pp. 1325–1348.
Seymour, R.S., Angove, S.E., Snelling, E.P., Cassey, P., 2015. Scaling of cerebral blood perfusion in primates and marsupials. J. Exp. Biol. 218, 2631–2640.
Seymour, R.S., Bosiocic, V., Snelling, E.P., 2016. Fossil skulls reveal that blood flow rate to the brain increased faster than brain volume during human evolution. R. Soc. Open Sci. 3, 160305. http://dx.doi.org/10.1098/rsos.160305.
Shettleworth, S.J., 2009. Cognition, Evolution, and Behavior, second ed. Oxford University Press, New York.
Šidák, Z., 1967. Rectangular confidence regions for the means of multivariate normal distributions. J. Am. Stat. Assoc. 62, 626–633.
Smith, R.J., Jungers, W.L., 1997. Body mass in comparative primatology. J. Hum. Evol. 32, 523–559.
Sokal, R.R., Rohlf, F.J., 1995. Biometry: The Principles and Practice of Statistics in Biological Research, Third ed. W. H. Freeman and Co., New York.
Stephan, H., Frahm, H., Baron, G., 1981. New and revised data on volumes of brain structures in insectivores and primates. Folia Primatol. 35, 1–29.
Strominger, N.L., Demarest, R.J., Laemle, L.B., 2012. The Human Nervous System: Structure and Function, Seventh ed. Springer, New York.
Tacutu, R., Craig, T., Budovsky, A., Wuttke, D., Lehmann, G., Taranukha, D., Costa, J., Fraifeld, V.E., de Magalhães, J.P., 2013. Human ageing genomic resources: integrated databases and tools for the biology and genetics of ageing. Nucleic Acids Res. 41, D1027–D1033.
Tatu, L., Moulin, T., Bogousslavsky, J., Duvernoy, H., 1996. Arterial territories of human brain: brainstem and cerebellum. Neurology 47, 1125–1135.
Tatu, L., Moulin, T., Bogousslavsky, J., Duvernoy, H., 1998. Arterial territories of the human brain: cerebral hemispheres. Neurology 50, 1699–1708.
Turnquist, J.E., Minugh-Purvis, N., 2012. Functional morphology. In: Bennett, B.T., Abee, C.R., Henrickson, R. (Eds.), Nonhuman Primates in Biomedical Research. Academic Press, Boston, pp. 87–129.
Vaishnavi, S.N., Vlassenko, A.G., Rundle, M.M., Snyder, A.Z., Mintun, M.A., Raichle, M.E., 2010. Regional aerobic glycolysis in the human brain. Proc. Natl. Acad. Sci. 107, 17757–17762.
van Bel, F., Roman, C., Klautz, R.J.M., Teitel, D.F., Rudolph, A.M., 1994. Relationship between brain blood flow and carotid arterial flow in the sheep fetus. Pediatr. Res. 35, 329–333.
Van Valen, L., 1974. Brain size and intelligence in man. Am. J. Phys. Anthropol. 40, 417–423.
Waschke, K., Schrock, H., Albrecht, D., Van Ackern, K., Kuschinsky, W., 1993. Local cerebral blood flow and glucose utilization after blood exchange with a hemoglobin-based O2 carrier in conscious rats. Am. J. Physiol. Heart C 265, H1243–H1248.
Weisbecker, V., Goswami, A., 2010. Brain size, life history, and metabolism at the marsupial/placental dichotomy. Proc. Natl. Acad. Sci. 107, 16216–16221.
Wellens, D.L., Wouters, L.J., De Reese, R.J., Beirnaert, P., Reneman, R.S., 1975. The cerebral blood distribution in dogs and cats. An anatomical and functional study. Brain Res. 86, 429–438.
White, L.E., Cant, N.B., 2016. A Laboratory Guide for Learning Functional Human Neuroanatomy. Duke Institute for Brain Sciences, Durham, NC.
Wible, J.R., 1993. Cranial circulation and relationships of the colugo *Cynocephalus* (Dermoptera, Mammalia). Am. Mus. Novit. 3072, 1–27.
Willerman, L., Schultz, R., Rutledge, J.N., Bigler, E.D., 1991. In vivo brain size and intelligence. Intelligence 15, 223–228.